Uncovering the mechanism of CD2AP behind Alzheimer's disease

TIAGO MIGUEL PICONÊZ PEREIRA

A dissertation submitted in partial fulfillment of the requirements for the Degree of Masters in Biomedical Research (Specialization Area: Regenerative Medicine) at Faculdade de Ciências Médicas | NOVA Medical School of NOVA University Lisbon

September, 2022

UNCOVERING THE MECHANISM

OF CD2AP BEHIND ALZHEIMER'S DISEASE

Tiago Miguel Piconêz Pereira
Supervisor: Cláudia G. Almeida, Principal Investigator
Nova Medical School (NMS), Universidade Nova de Lisboa

A dissertation submitted in partial fulfillment of the requirements for the Degree of Masters in Biomedical Research (Specialization Area: Regenerative Medicine)

September, 2022

FUNDING

This project has received funding from Marie Curie Integration Grant (PCIG-GA-2012-334366-trafficinAD; Marie Curie Actions, EC); iNOVA4Health—UID/Multi/04462/2019, a program financially supported by Fundação para a Ciência e Tecnologia (FCT)/ Ministério da Educação e Ciência, through national funds and co-funded by FEDER under the PT2020 Partnership Agreement); Maratona da Saúde 2016; Investigator FCT (IF/00998/2012, FCT); CEECIND/00410/2017 financed by FCT; ALZ AARG-19-618007 Alzheimer's Association; from the research infrastructure PPBI-POCI-01-0145-FEDER-022122, co-financed by FCT (Portugal) and Lisboa2020, under the PORTUGAL2020 agreement (European Regional Development Fund); the European Union's Horizon 2020 research and innovation program under grant agreement No 811087 (Lysocil).

Acknowledgments

I dedicate this thesis to my colleagues, friends, professors (who I also see as dear friends), and family. Without you, this amazing journey that started two years ago would not be the same. You all inspired me to grow, be more confident, and, most importantly, have fun doing science and thinking science.

Cláudia and Rita Teodoro, you are the ones who inspire me to grow and improve as a scientist.

Cláudia, I am grateful to have been given the opportunity to have someone with such knowledge and a sharp critical thinking, mentoring me. I thank you for allowing me to grow, for giving me the freedom to think and test my hypothesis while always being always there, shaping my mind and language in a more scientific manner. I feel fortunate, not only because I had the luck to have you as my mentor, but also because I could be myself and be at ease talking with you, thank you for your kindness and positivity. I apologise for my innate stubbornness; however, I will take our scientific discussions as my favourite moments during the Master thesis. It was an absolute pleasure to discuss science with you.

Thank you, Rita, for encouraging, motivating, and being the amazing teacher that we, the NBR students, needed. Our conversation on fighting anxiety and making that extra effort to speak in public was the driving force behind my public speaking efforts.

I also thank Paulo Pereira, Cláudia, and Rita for creating this Master's focused on our career development in science.

To my lab mates, thank you, Mariana, for teaching me how to work with cell culture. I also thank Tatiana, Jorge, and Raquel for making me feel welcomed, for always being there whenever I needed help, for the patience and for answering my not-so-smart questions whenever they popped up! I feel that I never ran out of these types of questions, so I hope you got used to it. A special thanks to you, Tatiana, through finishing your PhD thesis and submitting your paper, you never said no to helping others, and somehow, you always managed to create time to help who ever needed your assistance. I want you to know that you inspired me to become as autonomous and talented as you one day.

I thank the CEDOC Institute for giving me the tools to develop my thesis project.

Thank you, Marta and Catarina, two students I had a lot of fun training and answering your not-so-smart questions. It was a pleasure to be able to teach you what once, my colleagues have taught me. Hopefully, we will see each other again doing science.

To all my friends of the NBR, thanks for all the support, dinners, games, and good times. In particular, a big thanks to you, Dinis, Joana, Carolina, Rita, Mauro, Maria, and Patricia. Without you, this journey would not be the same, you have inspired me to keep pushing forward, even when it seemed difficult. I can't wait to see what you will conquer in the future.

To my friends, the "Mulas de Cascais", I am incredibly grateful for having you on my side, worrying about my wellbeing, constantly lifting me, and always curious about my work. Thank you, Daniel, Mariana, Raquel, and Sandro. You guys were my rock.

Totopo, although slightly more distant geographically, I also thank you for all the support and for always giving me your top bits of advice. I am grateful to have you, and I miss you a lot.

Um obrigado de coração aos meus pais e irmão. Sem vocês nada disto seria possivel. Obrigado por acreditarem em mim e deixarem-me sonhar.

Abstract:

Alzheimer's Disease (AD) is the most common form of dementia, where the key initiator is the excessive production of amyloid beta (Aβ). Aβ production from the processing of amyloid precursor protein (APP) by BACE1 and γ-secretase happens on the membrane of the endosomes when APP is not sorted for lysosomal degradation. Previously, CD2-associated protein (CD2AP), an AD genetic risk factor, was implicated in endocytic trafficking and actin cytoskeleton dynamics. In neurons, CD2AP promotes APP endosomal sorting for degradation and, thus, regulates amyloid beta production. However, whether the regulation of F-actin by CD2AP is required for APP sorting is unknown. Previous work found that interfering with the Actin-Related Protein 2/3 (ARP 2/3) complex containing the ARPC1A isoform may recapitulate the loss of endosomal F-actin induced by CD2AP depletion. We hypothesize that the ARP 2/3 complex containing the ARPC1A isoform acts with the CD2AP to stabilize endosomal branched F- actin to mediate APP endosomal sorting.

Using N2a cell line transfected with siRNA against CD2AP or the ARPC1A isoform, together with immunofluorescence, trafficking assays, and live imaging, we found that ARPC1A loss of function leads to a specific decrease in perinuclear F-actin in a likewise manner to CD2AP loss of function. Importantly, ARPC1A was found to regulate CD2AP perinuclear localization and levels. In agreement, CD2AP enrichment on endosomes was found more associated with ARPC1A than ARPC1B isoform. Moreover, CD2AP dynamics may be impaired with the downregulation of ARPC1A. ARPC1A loss of function delayed the degradation of APP to the same extent as CD2AP loss of function. Moreover, the loss of function of ARPC1A affects the early endosomes, decreasing EEA1 signal, endosome size, and endosomal APP.

In conclusion, our results indicate that CD2AP is recruited to early endosomes by ARP2/3/1A subcomplex dependent-branched F-actin polymerization to stabilize endosomal branched F- actin, which is necessary to mediate APP endosomal sorting for degradation.

Key words: Alzheimer's Disease, Intracellular trafficking, CD2AP, actin cytoskeleton, Arp 2/3 complex

Resumo:

A doença de Alzheimer (AD) é a forma mais comum de demência em que a causa principal é a produção excessiva de beta amiloide (Aβ). A produção de Aβ a partir do processamento da proteína precursora amiloide (APP) pela BACE1 e γ-secretase, ocorre na membrana dos endossomas quando a APP não é sujeita à seleção para a degradação lisossomal. Anteriormente, a proteína associada à CD2 (CD2AP), um fator de risco genético associado à AD, implicado no tráfico endocítico e na dinâmica do citoesqueleto de actina. foi implicado na seleção do APP endosomal para degradação e, portanto, na regulação da produção beta amiloide, no entanto, desconhece-se se a regulação da F-actin pelo CD2AP é necessária para a discriminação do APP. Trabalhos anteriores descobriram que o silenciamento do complexo Actin Related Protein 2/3 (ARP 2/3) contendo a isoforma ARPC1A pode recapitular a perda de F-actin endosomal induzida pelo decréscimo do CD2AP. Colocamos em hipótese, que o complexo ARP 2/3 contendo a isoforma ARPC1A, atua com o CD2AP para estabilizar a F-actina ramificada dos endossomas para mediar a seleção endosomal APP.

Utilizando a linha celular N2a transfectada com siRNA contra CD2AP ou a isoforma ARPC1A, juntamente com imunofluorescência, ensaios de tráfico e microscopia, descobrimos que a perda de função ARPC1A leva a uma diminuição específica da F-actin perinuclear de forma semelhante à perda de função CD2AP. É importante notar que o ARPC1A foi encontrado a regular a localização e níveis perinucleares de CD2AP. De acordo, o enriquecimento de CD2AP em endossomas foi encontrado mais associado à ARPC1A do que à isoforma ARPC1B. Além disso, a dinâmica CD2AP pode ser prejudicada com a desregulamentação do ARPC1A. A perda da função ARPC1A atrasou a degradação do APP na mesma medida que a perda da função CD2AP. Além disso, a perda de função da ARPC1A afeta os endossomas precoces, diminuindo o sinal EEA1, o tamanho dos endossomas e o APP endosomal.

Em conclusão, os nossos resultados indicam que o CD2AP é recrutado para endossomas precoces pela polimerização dependente do complexo ARP2/3 contendo a isoforma ARPC1A, para estabilizar a actina F-ramificada endosomal, que é necessária para mediar a separação endosomal do APP para a degradação.

Palavras-chave: Doença de Alzheimer, Tráfico Intracelular, CD2AP, Citosqueleto de actina, complexo Arp 2/3

I. TABLE OF CONTENTS

List of figures

III. Results

List of Tables

List of Abbreviations

α-CTF: α-cleaved C-terminal fragment

β-CTF: β-cleaved C-terminal fragment

Aβ: beta-Amyloid

ABP: Actin-binding protein

AD: Alzheimer's Disease

APP: Amyloid precursor protein

IP: Immunoprecipitation

ARP 2/3 complex: Actin-related protein 2/3 complex

BACE1: β-secretase-1

BBB: Blood-Brain barrier

CCP: Clathrin-coated pits

CC: Coiled coil

CD2AP: CD2-associated protein

CP: Capping protein

EEA1: Early-endosome antigen 1

EGF: Epidermal growth factor

EGFR: Epidermal growth factor receptor

EOAD: Early-onset Alzheimer's Disease

ESCRT: Endosomal sorting complex required for transport

F-actin: Filamentous actin

FDA: Food and Drug Administration

FRAP: Fluorescence Recovery after Photobleaching

G-actin: Globular actin

LAMP1: Lysosomal-associated membrane protein 1

LOAD: Late-onset Alzheimer's Disease

MPR: Mannose 6-phosphate receptor

MVB: Multivesicular body

Myo1: Myosin 1

N2a: Neuro2a

NMDA: N-methyl-D-aspartate

NPF: Nucleation-promoting factor

N-WASP: Neuronal Wiskott-Aldrich Syndrome protein

Rab5QL: Rab5(Q79L)-Myc

RIN3: Ras And Rab Interactor 3

sAPPα: soluble APPα

siRNA: small interference RNA

SH3: src homology 3

tfnR: Transferin receptor

TGN: trans-Golgi network

I. INTRODUCTION

I.1 ALZHEIMER'S DISEASE

I.1.1 History of Alzheimer's Disease

In 1907, a 51-year-old patient was observed by Alois Alzheimer. A german neuropathologist was invited to join Emil Kraepelin's Institution in the asylum of Frankfurt am Main. Alois described this patient as showing signs of memory loss, confusion, and complete dependence. Four years later, the patient died, and the postmortem analysis showed brain atrophy, an abnormal decrease in the number of neurons in the cortex, and what was described as "*minute miliary foci which are caused by the deposition of a special substance in the cortex"*(Stelzmann et al., 1995; Zhagn & Li, 2014). Today we term these miliary foci as amyloid plaques (Masters et al., 1985) composed of amyloid-beta (Aβ), a small peptide with a high susceptibility to aggregate extracellularly (Glenner, G. and Wong, 1984; LaFerla et al., 2007).

This description was further amplified in the eighth edition of Kraepelin's "*Textbook of Psychiatry"* (Schorer, 1985), where Kraepelin named the condition Alzheimer's Disease honouring Alois' discovery and doing a detailed description of the development of the disease over the patient's lives. In this detailed characterization, Kraepelin started by illustrating the first degenerative signs where patients would have unnoticeable symptoms, such as simply mistaking people's faces, not feeling right anymore, or becoming confused, escalating to agitated behaviour. At this point, the patients start to mutter to themselves, sing, laugh, and run around, but at the same time, they would not understand directions, objects, or pictures. Hereafter, the patient's speech starts to deteriorate rapidly. In the beginning, they can still frequently express themselves with occasional occurrences of meaningless and toneless chatter, but later on, the communication further deteriorates into a completely incomprehensible succession of babbling syllables.

In the last stages of the disease, the most severe symptoms of dementia develop. The patient becomes mute, only responding to the excitement with a senseless group of words. Patients no longer understand words or facial expressions and respond to confrontations with gestures of irritation. Moreover, patients also become dependent, unable to care for or feed themselves. The post-mortem findings, as issued by Alois Alzheimer's description, indicate unusually numerous extents of amyloid plaques and a loss of one-third of cortical cells, which in their place, they observe the presence of neurofibrillary tangles as the last residue of the dead cortical cells.

I.1.2 Epidemiology

Today, more than 100 years after the first case description, Alzheimer's Disease (AD) became the most common cause of dementia, affecting 30% of the population over the age of 85 years old. AD is also the fifth leading cause of death for those aged 65 or older, and as such, the total estimated worldwide cost of dementia in 2019 was over €1.2 Trillion. ("2020 Alzheimer's Disease Facts and Figures," 2020; *Estimates of Funding for Various Research, Condition, and Disease Categories (RCDC)*, 2021; Association, n.d.) Of note, although dementia mostly affects people over the age of 65, it is not part of normal aging (Irwin et al., 2018).

AD can be classified into two types that, although share the same brain pathological hallmarks, namely intracellular neurofibrillary tau tangles and extracellular Aβ plaques, they differ in the age of onset of the disease (Bertram & Tanzi, 2005).

Early onset AD (EOAD) starts before age 65, accounting for less than 5% of all AD cases, where the etiology resides in hereditary monogenic defects (B. L. Tang, 2009; Van Cauwenberghe et al., 2016). Some EOAD-associated mutated genes include amyloid-precursor protein (APP), presenilin 1, and presenilin 2, which are components of the γ-secretase complex required to produce Aβ (Mario F. Mendez, M.D., 2018).

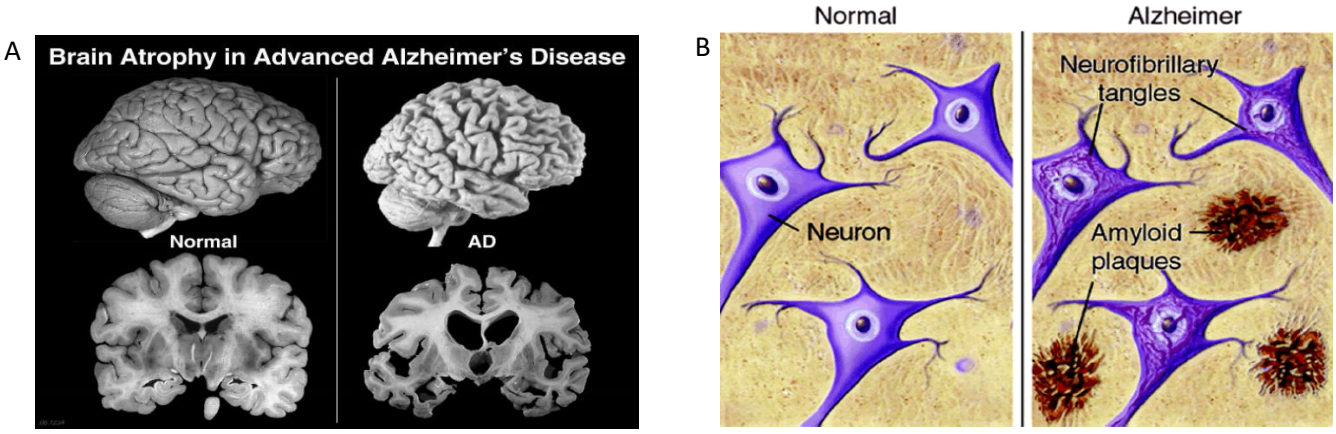

Figure 1.1 – Neuropathological features of Alzheimer's Disease.
*(**A**). Brain comparison between normal aging and AD figure obtained from Morales et al, 2010*
***B**). Cellular hallmarks of AD consisted of intracellular neurofibrillary tangle and extracellular amyloid plaques. Figure obtained from Mcgirr et al., 2020*

Most cases are associated with Late-Onset AD (LOAD), which is more prevalent after age 65. LOAD is a more complex disease with heterogeneous etiology, where aging, genetic risk factors, lifestyle, and metabolism contribute to the development of LOAD (Rabinovici, 2019). However, despite its complex characterization, LOAD has an estimated heritability of 60-80% (Carmona et al., 2018). As a result, genome-wide association studies looked at the allele frequencies of polymorphisms and identified LOAD susceptibility genes, including CD2-Associated Protein (CD2AP), as one of the top risk genes associated with LOAD (Hollingworth et al., 2011; Kunkle et al., 2019; Vardarajan et al., 2015).

I.1.3 Alzheimer's Disease treatment and the present caveats

Until recently, the therapies available concerning AD focused only on delaying the onset of symptoms, as there was no current treatment capable of stopping or reversing the pathology (known as disease-modifying therapies). These symptomatic approaches subdivide into three different groups: Cholinesterase inhibitors, the N-methyl-D-aspartate (NMDA) antagonist, and serotonin reuptake inhibitors (Yiannopoulou & Papageorgiou, 2013).

Cholinesterase inhibitors act on the synaptic cleft, delaying the degradation of acetylcholine, and thus, they enhance cholinergic transmission (Bartus RT et al., 1982; Cummings & Back, 1998). This group of drugs consists of donepezil (Pfizer), rivastigmine (Novartis), and galantamine (Janssen) and is used for first-line treatment of mild AD, showing a positive effect on slowing the decline in cognitive function.

A therapeutic option for moderate to severe AD is memantine (Lundbeck), an NMDA antagonist designed to protect neurons from excitotoxicity (Keating, 2011).

While cholinesterase inhibitors and memantine aim to preserve cognitive functions, a third group treats psychological symptoms of dementia, where 64% of patients with dementia suffer from hyperactivity (e.g., aggression) and 64% suffer from apathy. The most efficient antidepressants used to treat comorbid depression in AD are serotonin reuptake inhibitors (Mdawar et al., 2020; Sepehry et al., 2012).

On 7 June last year, the US Food and Drug Administration (FDA) approved aducanumab (Biogen), the first drug with a disease-modifying mechanism for AD. Aducanumab is a monoclonal antibody that selectively binds to soluble and insoluble aggregated Aβ (Schneider, 2020). In an early phase, Aducanumab was revealed to reduce amyloid plaques in a dose and time-dependent manner, with half of the patients who received the higher dose no longer presenting positive amyloid plaques after 12 months of treatment. Unfortunately, the delay in cognitive decline was very limited, and the secondary effects, such as edema and microhemorrhages, called Amyloid-related imaging abnormalities (ARIA), are significant, often causing headache, confusion, dizziness, and nausea (further detailed in (Lalli et al., 2021; Mukhopadhyay et al., 2021)).

I.2 Aβ INTRACELLULAR ACCUMULATION AND AMYLOID-PRECURSOR PROTEIN TRAFFICKING

Aβ intracellular accumulation is the earliest known mechanism triggering the onset of AD (Glenner, G. and Wong, 1984). Aβ is composed of several length-variants from 37 to 49 amino acids, being $A\beta_{37}$ and $A\beta_{38,}$ the two most abundant physiological isoforms, and $A\beta_{40}$ and $A\beta_{42,}$ the most pathological (Vadukul et al., 2017). The cytotoxic effects derived from $A\beta_{40-42}$ reside in the aggregation propensity, forming oligomers and amyloid fibrils (Braun et al., 2022; Kayed et al., 2003; Vadukul et al., 2017)

These variants are produced by the sequential proteolytic cleavage of the amyloid precursor protein (APP) (Selkoe DJ., 1998). However, despite the associated reputation of its degradation product for neurodegeneration, APP possesses a fundamental physiological function.

APP is a ubiquitously expressed transmembrane protein that contains a large extracellular N-terminal domain and a short C-terminal cytoplasmatic domain (O'Brien & Wong, 2011; Reinhard et al., 2005). APP expression is up-regulated in neurons, particularly during neuronal differentiation and maturation (Müller & Zheng, 2012), regulating neuromuscular junction formation, synapses, and dendritic complexity. APP also has an essential function in memory formation, being involved in neuritic outgrowth, synaptic pruning, and synapse plasticity (Kamenetz et al., 2003; Ludewig & Korte, 2017; Montagna et al., 2017). Interestingly, despite the knockout of the APP family of proteins results in perinatal death, this absence after development does not induce any cortical neurodegeneration (Arancio, 2020; Lee et al., 2020; Oh & Troncoso, 2014).

I.2.1 Molecular Mechanism of Amyloid-beta production

As part of the proteostasis equilibrium, all proteins are synthesized and eventually degraded, being APP no exception, with its processing increasing as we age (Burrinha et al., 2021).

After being produced, APP is transported from the Trans-Golgi-Network to the cell surface or to the early endosomes (EE), a process mediated by clathrin. At the cell surface, APP can be processed by the non-amyloidogenic pathway, being cleaved by the α-secretase and subsequently by the γ-secretase, a process that will release an APP C-terminal fragment (α-CTF) and a soluble APPα (sAPPα). The release of this soluble protein confers neuroprotective functions inhibiting neuronal apoptosis and increasing neuronal resistance to brain injuries (Müller et al., 2017).

Alternatively, APP can enter the amyloidogenic pathway, being endocytosed in clathrin-coated pits at the cell membrane into early endosomes. This step is augmented by synaptic activity (Cirrito et al., 2005; Small & Gandy, 2006) and aging (Burrinha et al., 2021). At this phase, APP can be processed by the transmembrane

protease β-secretase (BACE1), liberating the soluble form sAPPβ and β-CTF. β-CTF is cleaved by γ-secretase, generating Aβ (O'Brien & Wong, 2011).

Interestingly, the first evidence of Aβ being produced and secreted by cells was drawn by Koo and colleagues (1994), demonstrating that the internalization of cell surface APP generates Aβ via the coated pit-mediated endocytic pathway and then processed and released to the extracellular space (Koo & Squazzo, 1994). Of note, Aβ can also be processed by BACE1 at the Trans-Golgi network (TGN), mainly in neuronal cell lines (Seubert et al., 1993; Jun Zhao et al., 1996)

However, the encounter of APP with BACE1 on early endosomes is limited under physiological conditions. Two main controlling points explain this. The rapid recycling of BACE1 from the endosomes to the plasma membrane and APP sorting for degradation through intraluminal vesicles, in a process known as multivesicular body (MVB) biogenesis, and subsequent fusion with lysosomes (Clague & Urbé, 2008; Guimas Almeida et al., 2018) hindering the processing of APP. In addition to this, during physiological conditions, Aβ accumulation is further reduced as a result of the APP processing by α-secretase on the cell membrane, cleaving within the Aβ sequence and thus, precluding Aβ formation (Burrinha & Cláudia, 2022).

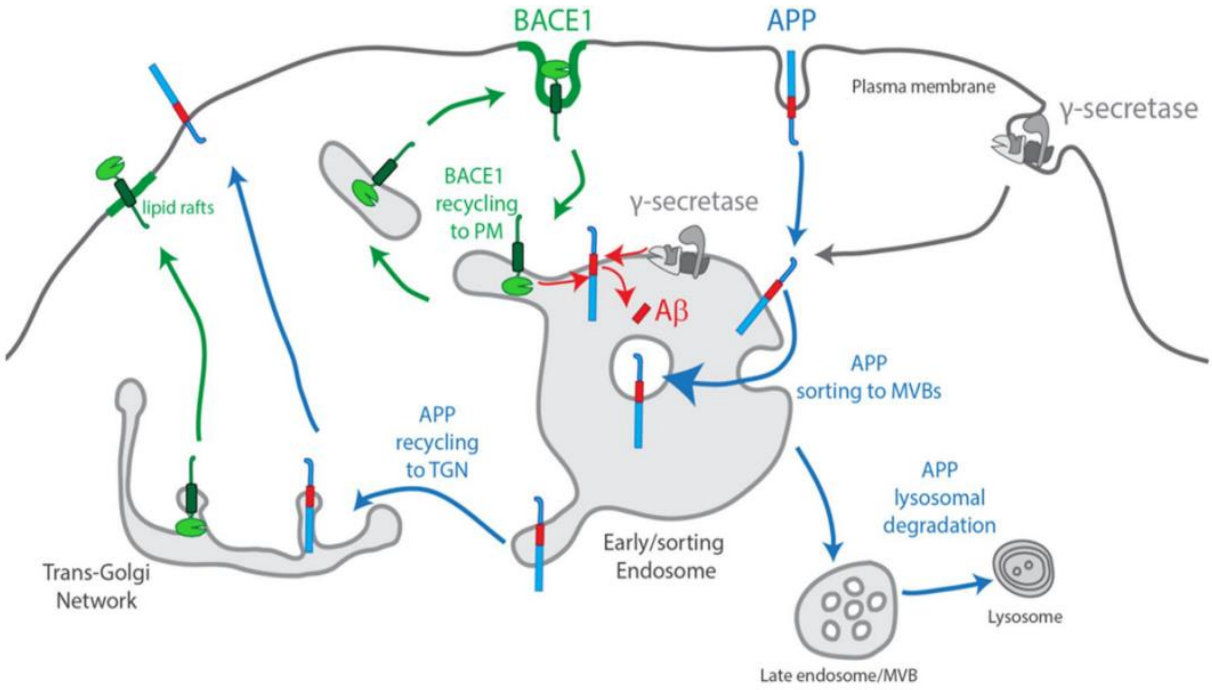

Figure 1.2 - APP endosomal processing.
APP and γ-secretase (BACE1) are separately endocytosed from the plasma membrane to the early endosomes. Here, APP can be processed through the non-amyloidogenic pathway, where APP is cleaved by α-secretase and γ-secretase and is subsequently sorted for lysosomal degradation. Alternatively, APP can be processed by the amyloidogenic pathway. Here, APP is cleaved by BACE1 and γ-secretase, releasing the insoluble Aβ peptide. Figure obtained from (Guimas Almeida et al., 2018)

I.3 CD2-Associated Protein

I.3.1 Structure

CD2-Associated protein (CD2AP) is an 80 kDa adaptor protein identified as one of the risk genes associated with LOAD (Lambert et al., 2013). Originally identified as interacting with the T-cell adhesion protein CD2, CD2AP is a ubiquitously expressed protein (Pawson & Scott, 1997; Wolf & Stahl, 2003).

Structurally, CD2AP is composed of three Src homology 3 (SH3) domains in the N-terminal, followed by a proline-rich region and a coiled-coil domain at the C-terminus. As an adaptor protein, the different domains of CD2AP grant its ability to bind and interact with several target proteins. Through the first two SH3 domains, CD2AP can interact with Ras and Rab Interactor 3 (RIN3), a Rab5 effector that enables CD2AP recruitment to early endosomes (Rouka et al., 2015; Shen et al., 2020). CD2AP interacts with cortactin and capping protein, two cytoskeleton proteins, via the Proline-rich domains. CD2AP interacts with F-actin and CapZ, an actin-binding protein, near the C-terminal domain, and via the coiled-coil domain, CD2AP can homodimerize. Lastly, CD2AP was found to interact with Rab4a, a GTPase (Monzo et al., 2005).

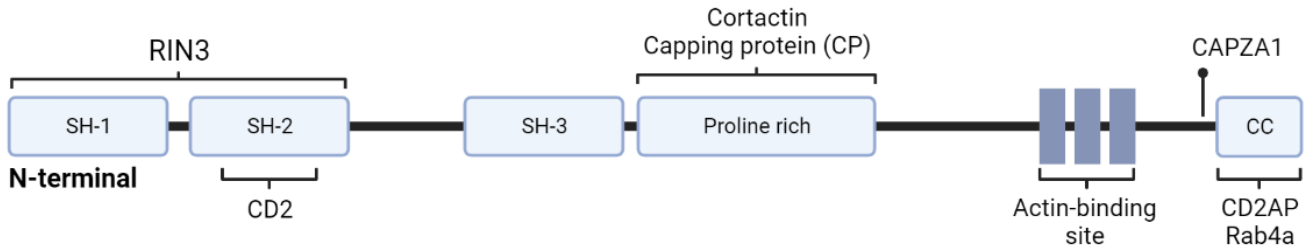

Figure 1.3: Schematic domain structure of CD2-associated protein (CD2AP).
CD2AP has three Src homology 3 (SH3) domains at the N-terminus, a proline-rich domain, and a coiled-coil domain (CC) with actin-binding sites at the C-terminus. Adapted from Monzo et al., 2005 and Rouka et al., 2015.

I.3.2 CD2AP functions in non-neuronal cells

CD2AP interaction with CD2 was initially described as required for CD2 clustering and CD2-dependent cytoskeletal polarization at the immunological synapse (Dustin et al., 1998). Later, CD2AP was also shown to regulate cell migration (Mustonen et al., 2005), actin cytoskeleton dynamic remodelling, and endocytic trafficking (Gauthier et al., 2007).

Although ubiquitously expressed, CD2AP occupies a determinant role in the processes of podocytes, a specialized type of epithelial cells localized around the glomerular capillaries in the kidney (Kobayashi, 2002; LI et al., 2000; Wolf & Stahl, 2003). CD2AP acts as an anchoring molecule, recruiting proteins to the podocyte foot junction and inducing signalling pathways. Indeed, CD2AP knockout (KO) mice die from nephrotic syndrome at six weeks of age. (Wolf & Stahl, 2003).

Moreover, Thilo Welsch et al. demonstrated that in podocytes, CD2AP colocalized with cortactin and F-actin on endosomal sorting vesicles, with CD2AP characterized by a high turnover and frequently associated with Rab4 but not Rab5 vesicles. Rab4 is a GTPase on early endosomes, responsible for balancing the vesicle traffic between the recycling and degradation pathways (Yang et al., 2016). Thus, CD2AP was hypothesized to be required for protein sorting into the degradative pathways and MVB formation (Welsch et al., 2005). Using Chinese hamster ovary (CHO) cells co-expressing CD2AP with Rab4, Cormont et al. revealed the formation of enlarged vesicles positive for EEA1 and Rab7 proteins enriched in early endosomes and late endosomes, respectively. These results suggested a role for CD2AP in early endosome morphology and regulating the early to late endosome transition (Cormont et al., 2003).

I.3.3 CD2AP function in Neuronal cells

Despite not being abundant in the brain, CD2AP was localized in the cerebrovascular endothelial cells by immunohistochemical studies (Allen brain Atlas; ID 12488). CD2AP mRNA was also detected on cortical and hippocampal neurons (Kirsch et al., 1999). Our lab showed that CD2AP was polarized to post-synaptic compartments and localized at the dendritic early endosomes (Ubelmann et al., 2017).

Through a transcriptomic screen, Harrison et al. identified CD2AP as a regulator of collateral sprouting, a mechanism by which neurons spared from a nervous system injury promote axon elongation (Harrison et al., 2016). CD2AP interaction with the nerve growth factor (NGF) receptor, a neurotrophic factor, was involved in regulating neuronal survival. More importantly, CD2AP colocalized with early endosomes identified by Rab5 (Harrison et al., 2016).

Recently, the CD2AP ortholog in flies, *cindr*, was likewise reported to play a function at neuronal synapses at the neuromuscular junction (Ojelade & M., 2019). By knocking down *cindr,* the authors revealed several neuronal defects, impairing synapse maturation and both synaptic vesicle recycling and release. Moreover, *cindr* was also shown to regulate the ubiquitin-proteasome system (UPS), thus affecting the turnover of synapsin, a synaptic protein (Ojelade & M., 2019).

I.3.4 CD2AP impact on the pathogenesis of Alzheimer's Disease

CD2AP regulation of blood-brain barrier integrity in endothelial cells

The blood-brain barrier (BBB) is a continuous endothelial membrane that surrounds the cerebral capillaries, which protects neurons from neurotoxic blood-derived products. The integrity of this barrier is thus vital for the brain's homeostatic environment, with the BBB breakdown and vascular degeneration promoting AD pathogenesis (Sweeney et al., 2018). APOE ε4, the most frequent risk factor for LOAD, was found to affect BBB integrity by reducing cerebral blood flow and increasing BBB leakiness (Halliday et al., 2016; Kim et al., 2011). Additionally, mice lacking CD2AP, except for the kidney and muscular cells, showed a reduced BBB integrity likely caused by the disruption of the adherens junctions and increased anxiety and motor defects (Cochran et al., 2015).

CD2AP regulation of APP Endocytic trafficking in neurons

CD2AP downregulation impairs APP degradation on dendrites due to a reduced transfer of APP from early to late endosomes (Ubelmann et al., 2017). Remarkably, while APP was enriched at the early endosome's lumen in wild-type primary neurons, ready to be degraded upon fusion with lysosomes, in CD2AP knockdown (KD) cells, APP was retained at the endosomal membrane. Downregulating CD2AP may decrease APP degradation by impairing APP endosomal sorting to the lumen, increasing the likelihood of APP converging with BACE1 to generate Aβ (Ubelmann et al., 2017).

In alignment, the overexpression (OE) of CD2AP accelerated the transfer of APP to late endosomes, increasing its degradation (Furusawa et al., 2019).

However, how CD2AP promoted the APP endosomal sorting was unclear. Given the several actin interaction domains of CD2AP, we hypothesise that CD2AP promotes APP endosomal sorting through an actin-mediated process.

I.4 ACTIN CYTOSKELETON

I.4.1 History and fundamental actin polymerization processes

In 1864, Kühne extracted a "viscous protein" separated from muscle with an apparent high salt concentration, naming it "myosin" and considering it to be responsible for the rigor state of the muscle. This myosin present in the muscle was then later studied by Szent-Györgyi, discovering that the threads prepared from myosin B could contract with the addition of boiled muscle juice, identifying the active material in the muscle extract as ATP. Today, myosin B is known as myosin II, the myosin responsible for muscle contraction. During this discovery, Szent-Györgyi considered this observation "perhaps the most thrilling moment of my life." Soon Straub joined Szent-Györgyi's lab and, through an elegant series of experiments, was able to extract the actin molecule from the "myosin extract," renaming the previously identified myosin into actomyosin. Furthermore, Straub discovered that actin existed in two forms, a globular form, stable in the lack of salt that, in the presence of ions, would polymerize, generating the filamentous form (Gyorgyi, 1943).

Today, actin is considered one of the most abundant proteins, present in all eukaryotic cells (Pollard, 2016) and comprising three isoforms, α, β and γ-actin, with α-actin being muscle-specific (Garrels & Gibson, 1976; Herman, 1993). Actin molecules are present either as a globular monomer (G-actin) or as a filamentous polymer (F-actin), being each monomer of the F-actin bound to either ATP or ADP. The formation of F-actin, also known as polymerization, requires three sequential phases: A nucleation phase where G-actin aggregates into unstable trimers, producing an active centre. This step is the slowest, occurring most frequently with the help of other actin regulators. The second phase is elongation, characterized by the sequential addition of G-actin molecules to the ends of the forming filament, increasing its length. During this event, one of the terminal sides of the filament will have a higher rate of polymerization (barbed end) than the other (pointed end). Lastly, the termination phase consists of the acquired balance between the free pool of G-actin and the length of F-actin to maintain the filament stability, avoiding its depolymerization, that is, the sequential and rapid removal of G-actin monomers from the previously formed F-actin (Rottner et al., 2017; Schmidt & Hall, 1998).

As numerous cellular events occur, actin filaments are dynamically forming and dissolving to generate forces essential to cellular homeostasis (Figure 1.4).

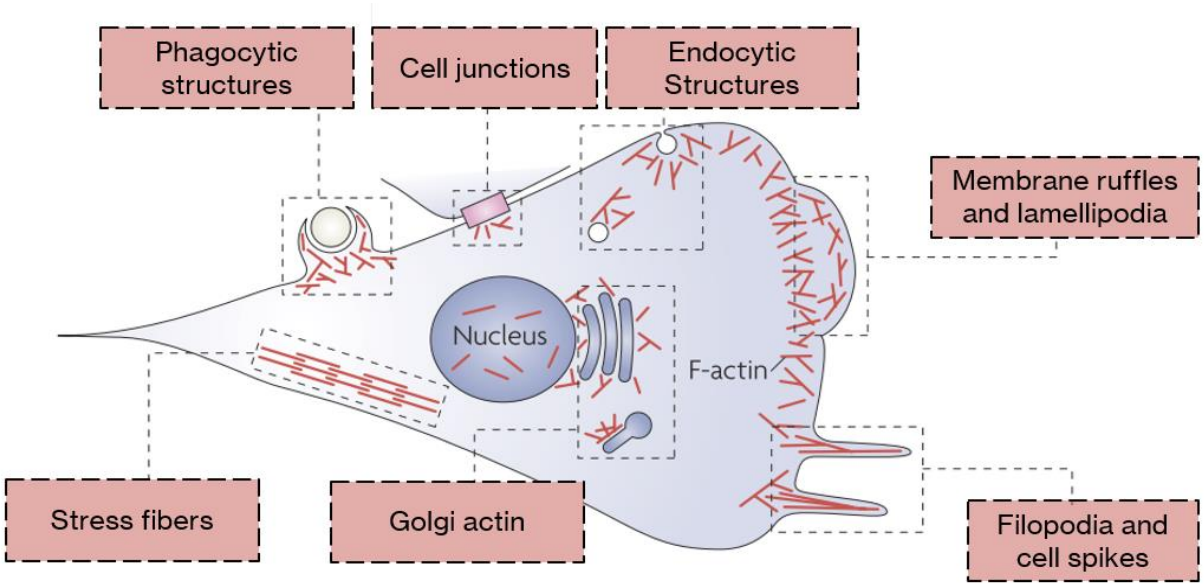

Figure 1.4 Subcellular distribution of F-actin.
F-actin (red) is nucleated and organized into branched networks by the Arp 2/3 complex or assembled into unbranched filaments by formins. Functional roles for different nucleation factors in a generic mammalian cell are depicted during phagocytosis, cell junction assembly, endocytosis, membrane ruffling and lamellipodia dynamics, filopodia formation, Golgi and tubulovesicular membrane dynamics, and stress fibre formation. Adapted from Campellone and Welch, 2010.

Mechanisms of actin polymerization

However, the polymerization process unveils far more complex than the three previous steps as purified actin isolated in a test tube is almost all polymerized in actin filaments having a slow filament assembly and disassembly. In contrast, only about half of the actin monomers exhibited are polymerized during physiological conditions, having a faster rate of filament assembly and disassembly (Pollard, 2016).

These fast actin dynamics are explained by the presence of the actin-binding proteins (ABPs), an ever-growing group of proteins capable of binding to actin and thus, regulating not only nucleation, elongation, and termination but also the disassembly, stability, and capacity to polymerize actin branches from previously established filaments (Figure 1.5) (Goode & Eck, 2007; Pollard, 2016). The major protein complex responsible for branched actin polymerization is the ARP 2/3 complex.

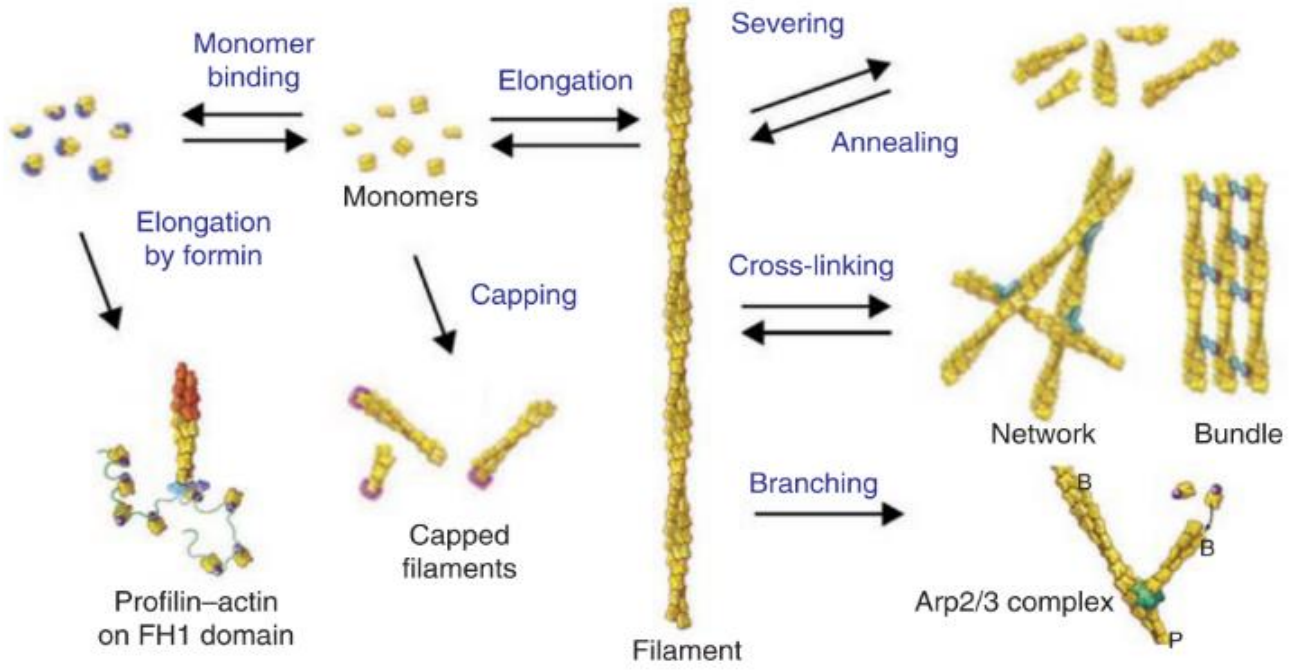

Figure 1.5 Mechanisms of F-actin regulation.
G-actin monomers can self-assemble forming actin filaments, a slow process known as spontaneous nucleation. However, through interaction with actin-binding proteins, actin nucleation can be facilitated by formins. Additionally, F-actin can also interact with other proteins to promote capping activity, branching, severing, annealing, and cross-linking. Figure obtained from *Pollard, 2016*

I.4.2 Arp 2/3 Complex

The Arp 2/3 complex consists of two Arps, the Arp2, and Arp3, with five additional subunits, known as ARPC1 to ARPC5. With little activity, the Arp 2/3 complex must be activated by Arp factors. Once activated, the Arp 2/3 initiates the formation of a branched F-actin (also known as daughter filament) in a y-branch configuration and recruits profilin to further increase daughter filament elongation through the ARP2 unit (Figure 1.6) (Goley & Welch, 2006).

I.4.2.1 Arp 2/3 isoforms

With an additional layer of complexity, some of the Arp 2/3 complex subunits also possess more than one isoform. While the central subunit ARP3 is ubiquitous, the isoform ARP3β is particularly enriched in neuronal cells, suggesting a role during brain development and maintenance (Jay et al., 2000).

The two subunits ARPC1 and ARPC5 were also present in two isoforms, ARPC1A and ARPC1B, and ARPC5 and ARPC5L. Through *in vitro* and cellular studies, the combination of the Arp 2/3 complex containing the ARPC1B and ARPC5L is more efficient in promoting actin polymerization with longer but less stable actin branches than its counterparts. Moreover, cortactin stabilizes ARPC1B/C5L-containing complexes over the ARPC1A/C5-containing complexes (Abella et al., 2016).

A recent study by Alexis Gautreau et al. on the function of the two ARPC1 isoforms in cell cycle progression uncovered significant differences between the two isoforms. ARPC1A distribution was found in dotty internal structures and colocalizing with the retromer complex, likely at the surface of endosomes, while ARPC1B was enriched at the lamellipodium. Furthermore, depletion of ARPC1A disrupted the formation of branched actin networks on endosomes, while depletion of ARP1B impaired the cortical actin network (Molinie et al., 2019).

Arp 2/3 mediated branching plays a vital role in several biological events, where the loss of Arp 2/3 function results in embryonic death and the absence of a single subunit isoform of the complex, ARPC1B, causing platelet abnormalities and leading to inflammatory disease in human patients (Kahr et al., 2017).

I.4.3 Nucleation-Promoting factors

Activation of the Arp2/3 is mediated by the nucleation-promoting factors (NPFs), essential molecules regulated by signal transduction, localized in cellular microdomains that orchestrate actin polymerization in a time and space-specific manner. These NPFs are further divided into classes: Class I and Class II.

Class I NPFs primary function is to mediate the association between free actin monomers and the Arp2/3 complex activating it. The Arp2/3 complex activation is mediated by a conformation change in the protein complex. Some of the most studied NPFs are the WAVE family, N-WASP and WASH. Among these, WASH regulates the sorting endosome, affecting both the recycling and degradative pathways (Harbour et al., 2012; Helfer et al., 2013).

Class II NPFs involve a less studied group of proteins. One of the Class II NPFs is cortactin, a protein that localizes to the cell cortex at lamellipodia (Kinley et al., 2003; Jianping Zhao et al., 2013) and endosomes (Muriel et al., 2016). Cortactin contains an Arp 2/3 binding domain at the N-terminal, a repetitive sequence able to interact with F-actin (Lynch et al., 2003). Furthermore, cortactin is considered to have a limited capacity to activate the Arp 2/3, being more important as a stabilizer of the actin branched network by increasing the association between the F-actin and Arp 2/3. Cortactin can also recruit other actin-binding proteins, such as CD2AP (Lynch et al., 2003) and CP, to increase filament stability and promote Arp 2/3 nucleation (Abella et al., 2016; Akin & Mullins, 2008).

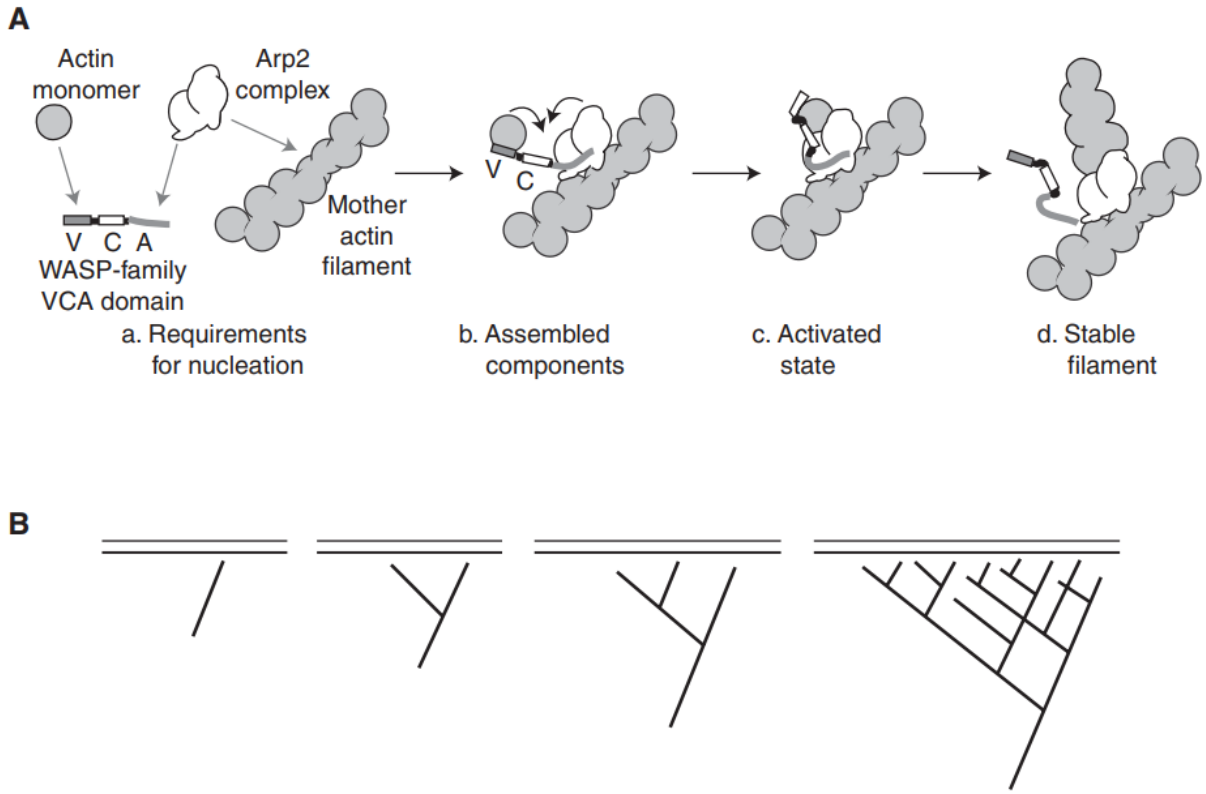

Figure 1.62 Mechanism of ARP 2/3 actin branched polymerization.
(A) Arp 2/3 complex links a pre-existing actin filament and a nucleator promoting factor (NPF) bound to an actin monomer. After assembly, the Arp 2/3 becomes activated, and changes in conformation. Lastly, the Arp 2/3 promotes the formation of a new filament attached to the side of the pre-existing filament and the NPF detaches, activating the Arp 2/3 somewhere else.
(B) The more branched actin is generated the higher the rate of the reaction, further stimulating Arp 2/3 nucleation. A process referred to autocatalytic branching. Figure obtained from R. Dyche Mullins, 2010.

I.4.4 Actin cytoskeleton dynamics in endocytic traffic

Consistent with the increasing knowledge of the diverse roles of actin in the cell, the actin cytoskeleton has been implicated in regulating endosomal trafficking, such as in clathrin-mediated endocytosis (Chakrabarti et al., 2021). Early yeast studies showed that actin is critical in regulating endocytic trafficking (Moreau & Winsor, 1997; Wendland et al., 1998). Actin and actin-binding proteins appear to regulate the initial steps of endocytic trafficking, as observed by the presence of cortical actin patches as sites of endocytosis in yeast (Kaksonen et al., 2003). These cortical patches are known to be produced by Arp 2/3 mediated branching and several Arp 2/3 activators (Schaerer-Brodbeck & Riezman, 2000). With each NPF showing a distinct behaviour, they most likely regulate different processes, ultimately leading to cargo internalization. One of the NPFs regulating protein is neural-WASP (N-WASP), colocalizing with Arp 2/3 at sites of clathrin-coated pits (CCP). Upon N-WASP depletion, a decrease in the endocytosis of epidermal growth factor (EGF), a molecule established to be endocytosed and undergo lysosomal degradation, was observed (Benesch et al., 2005).

Moreover, cortactin was detected during cargo internalization and mediating CD2AP recruitment to cortical actin through direct interaction, thus colocalizing CD2AP and cortactin to endocytosis (Jianping Zhao et al., 2013). CD2AP facilitates the recruitment of capping protein to cortactin, providing stability to the actin filaments at the cortex (Lynch et al., 2003). Actin polymerization inhibition using Latrunculin A, a toxin capable of binding to G-actin and disrupting F-actin, blocked CCP formation, establishing a role for actin polymerization during endocytosis (Merrifield et al., 2005).

As cargo internalization accumulates at CCP, a process known as vesicle budding, mechanical forces are exerted on the cell membrane generating curvature and turning it into a sphere, where dynamin resolves vesicle formation through scission. However, it recently was discovered that in stalled CCP, the Arp 2/3 complex and Cortactin, N-WASP, and F-actin promote asymmetrical actin assembly, facilitating a successful vesicle formation, independently of dynamin (Jin et al., 2022). The authors propose two exciting models. One where the local conditions favour membrane deformation, and thus, dynamin is sufficient to perform scission, and another where, due to higher membrane tension or other obstructions impeding membrane curvature, N-WASP activates Arp 2/3 asymmetrically on one side of the clathrin coat, generating asymmetric forces to free the vesicle from the plasma membrane.

Actin dynamics is also essential during early endosome maturation. Studies developed by Emmanuel Derivery, have found WASH complex to associate with endosomes through interaction with the retromer subunit, vacuolar Protein Sorting 35 (VPS35) (Harbour et al., 2012). WASH is reported to influence the shape and maturation of endosomes with WASH KO, causing the collapse of enlarged early endosomes devoid of F-actin (marked by the EEA1 protein, enriched in the early endosomal compartment) as well as a global collapse of

lysosomes (marked by LAMP1 enriched at late endosome and lysosomes). Additionally, WASH KO altered both retromer and degradative transport, demonstrated by the reduced levels of EGFR degradation and transferrin receptor (TfnR), respectively, demonstrating that WASH-mediated F-actin is indispensable for the integrity of both endosomal and lysosomal pathways (Derivery et al., 2009; Duleh & Welch, 2010; Gomez & Billadeau, 2009).

Moreover, in early endosomes, myosin I (Myo1), a protein capable of regulating membrane tension through actin architecture remodelling, has been implied in the degradative pathway promoting the endosomal sorting of cargo to the luminal multivesicular bodies (Salas-Cortes et al., 2005). Moreover, Almeida et al. described a function for Myosin 1b in the formation of tubules at the trans-Golgi network. Lastly, cortactin is also involved in the early endosomes, being required for endosome maturation and transfer through the degradative pathway, demonstrated by a reduced EGFR degradation in cells knockdown for Cortactin (Muriel et al., 2016).

Altogether, although the endosomal sorting complex required for transport (ESCRT) is identified as the core and indispensable machinery mediating cargo sorting for degradation, there is accumulating evidence of the contribution of F-actin dynamics regulated by several actin regulators that may mediate endosomal sorting for degradation independent of the ESCRT complex (MacDonald et al., 2018).

II. PROJECT HYPOTHESIS

CD2AP was shown to mediate APP lysosomal degradation through endosomal sorting. However, the mechanism by which CD2AP promoted the sorting of APP was unclear. Taking into consideration that:

1. CD2AP is an adaptor protein with multiple domains capable of interacting with F-actin and actin-binding proteins
2. Previous studies reported that F-actin dynamics on endosomes regulate events such as endosome maturation and both receptor recycling and degradation
3. We have previously observed that CD2AP knockdown may reduce F-actin patches on early endosomes

We intend to explore the CD2AP-mediated endosomal sorting mechanism, hypothesizing that this process is F-actin mediated with the assistance of other actin regulators.

To assess whether F-actin dynamics are required for the CD2AP-mediated sorting, we will analyse:

I. The impact of CD2AP loss of function in F-actin polymerization at the endosomal-rich perinuclear region
II. The impact of the ARPC1A isoform loss of function in perinuclear F-actin polymerization
III. The capacity of ARPC1A to regulate CD2AP localization and levels
IV. The effects of ARPC1A loss of function in APP trafficking

With this work, we expect to understand better how CD2AP promotes the sorting of APP and whether the ARPC1A-containing Arp 2/3 complex mediates this mechanism.

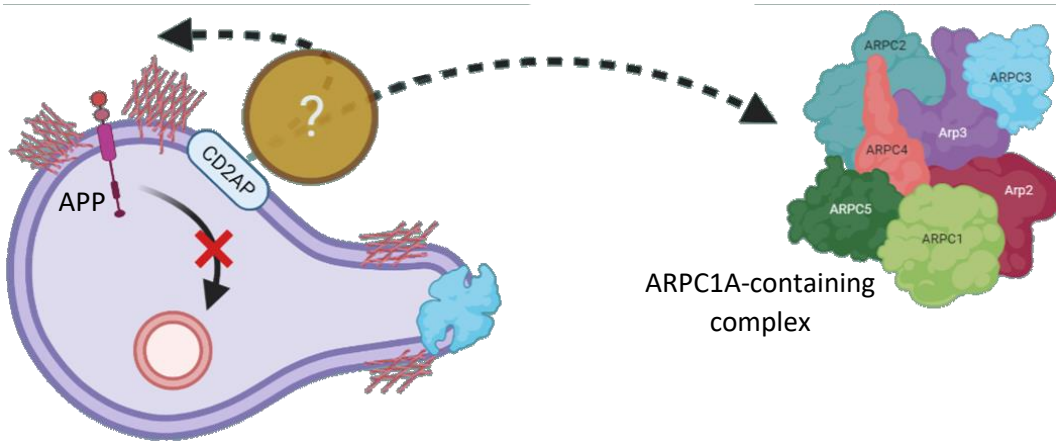

Figure 1.7 Hypothesis model for the mechanism of CD2AP-mediated sorting of APP. In normal conditions, CD2AP mediates APP endosomal sorting for degradation. Upon loss of CD2AP function, APP endosomal sorting becomes impaired, decreasing APP degradation and the F-actin colocalized with endosomes decreases. To evaluate the function of F-actin on endosomes, we targeted the ARPC1A-containing Arp 2/3 complex studying its role on endosomal sorting.

III. METHODS

III.1 CELL CULTURE

Neuro-2a (ATCC® CCL-131TM) is a *Mus musculus* brain neuroblastoma cell line established by R.J. Klebe and F.H. Ruddle, obtained from a spontaneous tumour of a strain A albino mouse (JAX stock #000646). N2a are adherent cells derived from neural crest mouse cells with a neuronal and amoeboid stem cell morphology and an unlimited proliferation *in vitro* (Tremblay et al., 2010).

Frozen cells (1ml) were quickly thawed and, in aseptic conditions, diluted in 9 ml of Dulbecco's Modified Eagle Medium (DMEM) (DMEM, GlutaMAXTM Supplement, GibcoTM, ThermoFisher Scientific) supplemented with 10 % fetal bovine serum (FBS) (Sigma-Aldrich) (complete medium). After centrifugation at 200x g, 2 minutes at room temperature (RT), the complete medium was replaced with 5 ml of fresh medium to remove dimethyl sulfoxide (DMSO), a cryoprotectant agent, present in freezing media but toxic at RT (Best, 2015). Cells were plated in a 25 cm T-flask (T-25, Sarstedt) in a humidified incubator at 37 ºC and 5 % CO2.

To maintain cells in culture, cells (90% of confluency) were rinsed with phosphate-buffered saline pH 7.4 (PBS) (GibcoTM, ThermoFisher Scientific) to remove serum that inhibits trypsin, and the culture medium was discarded. Trypsin-EDTA (0,25%) (1ml; with phenol red, GibcoTM, ThermoFisher Scientific) was added to dissociate and detach adherent cells for 2 min at 37 ºC and 5 % CO2. Trypsin activity was inhibited by adding complete medium to a final volume of 5 ml. Suspended cells were split 1:5 every other day or 1:10 every two days to maintain cell culture.

For experiments, suspended cells were diluted in Trypan Blue Solution, 0.4% 1:10 (Amresco®) labelling non-viable cells (Strober, 2001). Viable cells, not labelled with trypan blue, were counted using a Neubauer Counting Chamber (0.1mm, VWR, Marienfeld). To obtain the total number of cells per ml, the average number of cells in the eight grid squares in the Neubauer Chamber was multiplied by the dilution factor and the conversion factor for Neubauer (10^4). Then, N2a cells were plated differently depending on the aim of each experiment.

For immunofluorescence experiments, N2a cells were plated in 500 µL of complete media, in a 24-well plate in 13mm circular glass coverslips (VWR, Marienfeld), previously acid-washed and autoclaved. For immunofluorescence, 50×10^3 cells were plated, for siRNA experiments 25×10^3 cells were plated per well in a 24-well plate. For immunoblotting and biotinylation experiments, 100×10^3 cells were plated per well in a 6-well plate with 1,5mL of complete media. For live-imaging experiments, 120×10^3 cells for overexpression

experiments and 60×10^3 cells (for siRNA experiments, were plated in 1,5 ml of complete media in a 6-well plate with 25mm circular glass coverslips (VWR, Marienfeld), previously acid-washed and autoclaved.

For cryopreservation, cells were allowed to reach 75-80% confluence. Then, complete media was removed by centrifugation 200x g 5min at RT and replaced by DMEM, 20% FBS, and 10% DMSO. Cells were gradually stored at -20, -80ºC, and -150ºC.

III.2 TRANSFECTION

cDNA Preparation

A single colony from glycerol stock was selected using a sterile pipette tip and grown in 5 ml LB (Luria-Bertani) medium (LB Broth, Miller, Fisher BioReagentsTM, ThermoFisher Scientific) containing either ampicillin (100 µg/ ml) or kanamycin (100 µg/ ml), depending on the plasmid antibiotic resistance. Bacteria were incubated for 8 h at 37ºC with 225 rpm agitation. Then, the 5 ml culture was used to inoculate an Erlenmeyer containing 200 mL LB media supplemented with antibiotics depending on the antibiotic resistance present on the construct used. The 200 mL culture was incubated overnight at 37 ºC at 225 rpm. With the growth of bacteria confirmed by the presence of a cloudy haze in the culture media, DNA purification was performed using the ZYMidiprep/NZYMiniprep kit (NZYTech).

The precipitated DNA was dissolved in ultraPureTM DNase/RNase Free Distilled water (InvitrogenTM, Life Technologies) and the DNA concentration was determined using NanoDrop 2000 UV-Vis spectrophotometer (Thermo ScientificTM). To prepare a bacteria glycerol stock intended for long-term storage, 500 µl of bacterial culture was added to 500 µl of 50 % glycerol and stored at -80ºC.

Transient DNA transfection

For cDNA expression, we performed a lipid-based transfection based on the interaction of the positive surface charge of the DNA-lipid complex with the negatively charged cell membrane, thus enabling delivery of the cDNA to the cell via endocytosis, using lipofectamine 2000 (Thermo ScientificTM) according to the manufacturer instructions. First, DNA and lipofectamine 2000 were diluted separately in 12.5 µl of Opti-MEM Reduced Serum medium (GibcoTM, ThermoFisher Scientific). For the 6-well plate, the volumes used were proportional to the surface area. After 5 min incubation at room temperature (RT), the DNA mix was added to the diluted lipofectamine solution and incubated for 20 min at RT. The final DNA-lipid complex was added to the plated cells and incubated at 37 °C in a 5 % CO2 incubator for 24 h.

Cells were transfected with the following cDNA: pEGFP-C1 (Clontech), CD2AP-GFP (gift from Andrey Shaw, Washington University School of Medicine), CD2AP(K633R)-GFP, previously generated by site-directed mutagenesis (NZYTech) (primers:5'GAAATAGCAAAGCTGAAGAAAGCTGTTCTGTTG3' and 5'CAACAGAACAGCTTTCCTCAGCTTTGCTATTTC3'), Rab5(Q79L)-Myc (gift from M. Airpin, Institut Curie), APP-RFP (gift from S. Kins, University of Kaiserslautern), LifeAct-Cherry (gift from Dr. R. Wedlich-Söldner (MPI Biochem)). The Arp 2/3 subunits 1A, 1B, and C2-GFP (gift from Edgar Gomes, iMM).

Small interfering RNA transfection

For small interfering RNA (siRNA) treatment lipofectamine RNAiMax (Thermo ScientificTM) was used according to manufacturer instructions. Briefly, siRNA (5pmole) and lipofectamine RNAiMAX (0,8µl) were diluted separately in 25 µl of Opti-MEM medium (Optimem |Reduced Serum Medium, GibcoTM, ThermoFisher Scientific). After 5min of incubation at RT, the siRNA mix was added to the diluted Lipofectamine (1:1 ratio) and incubated for 20min. The cell culture media was removed to add 450 µl of complete media and the final siRNA-lipid complex (50µl) was added to the plated cells for a final siRNA concentration of 10-20nM depending on the siRNA. Cells were incubated at 37 ºC and 5 % CO2 for 72h.

Cells were transiently transfected with non-targeting control siRNA (ID: AM4611 ThermoFisher Scientific) and (GeneCust), siCD2AP (CD2AP siRNA (sc-29985, Santa Cruz Biotechnology), three different sequences of siARPC1 (s80580(#1), s80581 (#2) and s80582 (#3), ThermoFisher Scientific), ARPC1B (s76595, ThermoFisher Scientific) and ARPC2 (s94586, ThermoFisher Scientific).

For DNA and RNA transfection experiments, cells were first transfected with siRNA for 48h. cDNA was transfected as described above, and cells were analysed after 24h, for 72h of siRNA transfection.

III.3 IMMUNOFLUORESCENCE

N2a cells were quickly washed in PBS 1X and fixed in 4% paraformaldehyde (PFA) (Sigma-Aldrich) diluted in PBS 1X for 10 min. Cells were then washed twice with PBS 1X, permeabilized with 0.3% Triton X-100 (Merck) for 5 min, and then blocked in 0.1% saponin (Sigma-Aldrich), 1% bovine serum albumin (BSA; NZYTech) and 2% FBS (Sigma-Aldrich) in 1X PBS for 1h. After blocking, cells were incubated for 1 h at RT with primary antibodies (Table 1) in blocking solution, washed three times with PBS 1X, and incubated for 1h at RT in the dark with the appropriate secondary antibodies (Table 1). Finally, cells were washed three times with PBS, the

coverslips mounted on glass slides with Fluoromount-G mounting medium (Southern Biotech), and air-dried overnight.

Cell nucleus was labelled using DAPI (Sigma-Aldrich), a fluorescent dye with a strong interaction with adenine-thymine-rich regions in the DNA. F-actin was labelled using Phalloidin 647 (ThermoFisher Scientific) a fluorescently tagged molecule capable of binding and stabilizing F-actin.

Table 2.1 Antibodies and probes used in this work.

Antibody	Raised in	Recognizes	IF Dilution	Supplier
Primary Antibodies				
Anti-CD2AP	Rabbit	Human, Mouse, Rat	1:200	Sigma-Aldrich
Anti-EEA1	Mouse	Human, Rat	1:100	BD Transduction Laboratories
Anti-APP (Y188)	Rabbit	Human, Mouse	1:200	Genetex
Anti-c-Myc (9E10)	Mouse	Human, Mouse	1:200	ThermoFisher Scientific
Secondary Antibodies				
Anti-Rabbit	Goat	Rabbit	1:200	ThermoFisher Scientific
Anti-Mouse	Goat	Mouse	1:200	ThermoFisher Scientific
Probes				
DAPI	-	-	1:100	Sigma-Aldrich
Phalloidin-647	-	-	1:250	ThermoFisher Scientific

III.4 IMMUNOBLOTTING

Lysate preparation

After the appropriate treatment (siRNA or cDNA), cell culture media was removed, and cells were washed with ice-cold PBS. During lysate preparation, all the steps were performed on ice. Cells were lysed using 100 µl per 6-well plate of a modified Radio-Immunoprecipitation Assay (RIPA) lysis buffer (50 mM Tris-HCL pH 7.4 (Tris base, NZYTech), 150 mM NaCl, 1% NP-40 (Igepal CA-630, Sigma-Aldrich), 0.25% sodium deoxycholate (DOC) (≥97.0%, Sigma-Aldrich), 1mM EGTA (for molecular biology, ≥97.0%, Sigma-Aldrich), 0,1%-1% SDS (Sodium Dodecyl Sulfate, White Powder, Electrophoresis, Fisher Scientific)) and Protease Inhibitor Cocktail (PIC) 1X (stock 25X) (complete, EDTA-free Protease Inhibitor Cocktail, Sigma-Aldrich) added fresh.

After 5 min incubation with lysis buffer, cells were scrapped off using a plastic cell scraper. The cell suspension was transferred into a pre-cooled tube and incubated on ice for 15 min. Lastly, the cell lysate was centrifuged at 17 000x g, 15min at 4˚C, and the supernatant was either stored at -80˚C or used on the same day for protein analysis by SDS-PAGE and western Blot.

SDS-PAGE

After lysate preparation, (5µl) 4X LDS sample buffer (4X BoltTM LDS Sample Buffer, InvitrogenTM, NovexTM, ThermoFisher Scientific) was added to the cell lysate (15µl) for a final volume of 20µl. The mix was then incubated for 5min at 95˚C, followed by highspeed centrifugation.

Protein was separated by using Tris-Glycine SDS-polyacrylamide gel electrophoresis (SDS-PAGE) (running buffer: 25 mM Tris, 192 mM glycine (NZYTechTM), and 0.1% (w/v) SDS) at 100-120 V for 1h, using Mini-PROTEANTM. (BioRad).

Protein Ladder, ThermoFisher Scientific) was used to determine proteins molecular weight.

Protein transfer

Proteins separated were transferred to 0.45 µm nitrocellulose membranes (8.5×6.0cm) (GE Healthcare), using a wet transfer sandwich and the transfer system Mini BlotTM Module (InvitrogenTM, ThermoFisher Scientific), at 10 V for 1h with transfer buffer (20 mM Tris base (NZYTech), 150 mM Glycine (NZYTech), 0.04% SDS (Fisher Scientific) and 20% (v/v) ethanol 96%).

The transfer membrane was incubated with the Ponceau S solution (0,5% Ponceau S (Merck), 1% Acetic glacial 100% (anhydrous, Merck) to detect the proteins transferred (Ausubel et al., 2003) after appropriate washing with Milli-Q water.

Western Blot

The membrane was then blocked in 5% milk (Nestlé) in PBS-T (PBS with 0,01% of Tween 20 (Sigma-Aldrich)) for 1 h at RT. After blocking, the membrane was incubated with rabbit anti-APP (Y188) (Genetex) diluted in 1 % dry milk in PBS-T for 16 h at 4 ºC, with constant agitation.

Membranes were washed 4 times for 5 min in PBS-T and incubated with anti-Rabbit conjugated with horseradish peroxidase (HRP) in 1 % dry milk in PBS-T 1 h at RT with agitation. Following secondary antibody incubation, the membrane was washed 4 times for 5min with PBS-T.

Membranes were incubated with equal amounts of luminol and peroxidase solution for 1 min (enhanced chemiluminescence) (Amersham ECL 420 Prime Detection Reagent, GE Healthcare) to detect the target proteins. Images of immunoblots were captured using a ChemiDoc imager (BioRad) within the linear range. Quantification of densitometry was performed using Fiji (ImageJ), and band intensities of proteins of interest were normalized to the corresponding band intensity of α-tubulin or APP direct load depending on the experiment.

III.5 APP TRAFFICKING BIOTINYLATION ASSAY

Biotinylation

To assess APP degradation, N2a were plated on a 6-well plate. After 72 hours of siRNA transfection, cell culture media was removed, and N2a cells were washed twice with PBS 1X 0.1 mM $Ca^{2+}Mg^{2+}$. Next, cells were incubated with 600µl of biotin solution (0.5 mg/ml of Sulfo-NHSLC-Biotin (Pierce) in PBS 1X 0.1 mM $Ca^{2+}Mg^{2+}$) for 5min at RT. After, the reaction was quenched by removing biotin and washing cells three times with (600µL) 0.5% BSA in PBS 1X 0.1 mM $Ca^{2+}Mg^{2+}$ and once with PBS 1X 0.1 mM $Ca^{2+}Mg^{2+}$ alone. Cells were then either lysed (0min chase) and kept on ice or chased for 30 min and 60 min at 37˚C, adding pre-warmed complete cell culture media. After finishing lysate preparation for all time points, 15 µl of each lysate was stored at -80˚C for the direct load (DL), while the remaining was used for immunoprecipitation (IP).

Immunoprecipitation

For biotin immunoprecipitation, 30 µl of NeutrAvidin agarose beads (Pierce) in 200µL of lysis buffer was added to the IP lysate for 16 h at 4 ˚C with constant agitation. During this process, the receptor proteins previously bound to biotin during biotinylation will precipitate with the NeutrAvidin beads, thus enabling the isolation of biotinylated proteins at the cell surface from the remaining proteins in the cell.

After incubation, the IP lysate was centrifuged 17 000x g, 2 min at 4 ˚C three consecutive times, removing the supernatant each time and resuspending the pellet with 100µl of lysis buffer with 1% glycerol. Then, the IP lysate was centrifuged, discarding the supernatant, resuspending the pellet in PBS 1X 0.1 mM $Ca^{2+}Mg^{2+,}$ and centrifuging one last time. After centrifugation, a syringe was used to remove the supernatant and dry the IP beads (bound to the previously formed Biotin-Protein complex).

Western Blot

After immunoprecipitation and purification, 26µl of 2X LDS sample buffer was added to the IP beads. 4X LDS sample buffer (5ul) was added to the previously stored (15µl) DL lysate. The mixes from both IP and DL lysates were incubated for 5min at 95˚C followed by highspeed centrifugation DL and the IP (without the beads) supernatants were analysed by SDS-PAGE and western blot with anti-APP Y188 (1:1000).

APP levels detected in the IP were quantified normalized to the APP levels detected in DL, further normalized to the APP levels detected at 0 min.

III.6 IMAGE ACQUISITION AND SINGLE-CELL AND SUBCELLULAR ANALYSIS

III.6.1 Image acquisition

Epifluorescence microscopy was performed using a Zeiss Z2 upright widefield microscope, equipped with an AxioCam 506 mono, using the 63x/1.4NA Plan-Apochromat Oil immersion objective, Alexa fluor 488, Alexa fluor 555 and Alexa fluor 647 fluorescence filter sets.

Super-resolution confocal microscopy was performed using Zeiss LSM 980 Multiphoton Airyscan 2 (Carl Zeiss Ltd, Cambridge, UK) with a 63x objective (Figure 5). Fluorescence recovery after photobleaching (FRAP) experiments (Figure 8) was also performed using the LSM980 – Airyscan 2.0.

For direct comparison, samples were imaged using identical acquisition parameters.

Fluorescence Recovery After Photobleaching (FRAP)

N2a cells were transfected with CD2AP-GFP and LifeAct plasmids. For the imaging, cell culture media was replaced with live imaging media containing 120mM NaCl, 3mM KCl, 2mM $CaCl_2$, 2mM $MgCl_2$, 10mM Hepes and FBS (10%) and placed on the microscope environmental chamber at 37°C, 5% CO2.

A ROI corresponding to an area of the perinuclear region was bleached at maximum laser power (100%) and max scanning speed. Images of LifeAct-mCherry and CD2AP-GFP fluorescence before and after bleaching were obtained during the next 20 seconds at 1 second intervals until the fluorescence recovery stabilized. Images were taken by Zeiss LSM 980 - Airyscan and quantified with ImageJ using a FRAP analysis plugin developed by Jeff Lange at Stowers Institute.

III.6.2 Single-cell and subcellular analysis

Quantitative analysis

For perinuclear measurements (F-actin, CD2AP, and EEA1)(Figure 3.2B, 3.3B, 3.4C, 3.6B), images were analysed using the Icy Bio-image analysis software (Chaumont, F. et al. 2012). First, we outlined a region of the background using the tool “Rectangle selection” and measured the average fluorescence. Then, we outlined the whole cell using the “Polygon selection” tool and the perinuclear region using the “Ellipse selection” tool. The perinuclear region was identified as the cytoplasmatic region next to the nucleus, containing a cluster of F-actin, CD2AP or EEA1. The average intensity of the whole cell and perinuclear ROIs were measured.

Then, we subtracted the whole cell and perinuclear regions by the background, and subsequently, the total intensity of the whole cell and perinuclear region were calculated by multiplying by the respective ROI area. Finally, the total intensity of the perinuclear region was divided by the whole cell intensity and presented as the fraction of protein in the perinuclear region relative to the whole cell.

For CD2AP whole cell intensity (Figure 3.4B), the measurement of the average intensity of the whole cell was subtracted by the background and then normalized to the siControl. Results were shown as a percentage.

For the quantification of APP mean intensity in Rab5QL endosomes (Figure 3.7B), we used the Fiji tool "Polygon selection" to outline each RAB5QL endosome (ROI endosome). Then, the APP mean intensity was measured per ROI endosome. For each condition, results are shown in the percentage of siControl.

For the analysis of endosomal f-actin, endosomal CD2AP and EEA1 mean intensity (Figures 3.2C, 3.3C, 3.4D and 3.6C), we used the Fiji Comdet Plugin. Comdet plugin, is a tool that enables the segmentation and identification of foci signal, measuring each foci size (Figure 2.1 3A), foci intensity (Figure 2.1 3B), and colocalization (Figure 2.1 3C). First, we identified the region of interest using the "Oval selection" tool to outline the perinuclear ROI with 130x130 pixels. Then, we used the Fiji Comdet plugin to segment and identify the foci of interest in the perinuclear ROI. Lastly, the intensity of puncta identified from F-actin, CD2AP, and EEA1 channels were normalized to the siControl condition and shown as a percentage.

Similarly, for the analysis of APP intensity in EEA1 endosomes (Figure 3.6E.), we used the Fiji Comdet plugin, identifying as ROI, the perinuclear region and segmented the EEA1 vesicles. Then, for each punctum positive for EEA1 (Figure 2.1 3C) we extracted the intensity of APP (Figure 2.1 3A).

For the quantification of CD2AP and F-actin enrichment in endosomes (Figure 3.5C and 3.5G) we used the Fiji Comdet plugin. First, we used Fiji's "polygon tool" to outline the inner aspect of the Rab5QL endosomal membrane. Next, using the command "make a band", we expanded the line selection to a 0.35 um band that covered Rab5QL endosomal membrane (ROI membrane). We used the Comdet and measured the mean intensity of CD2AP puncta when colocalizing or not with ARPC1A/B. To obtain the CD2AP enrichment per ARPC1A/B puncta, we divided the intensity of CD2AP colocalized with ARPC1A/B by the intensity of CD2AP puncta alone (Figure 5I).

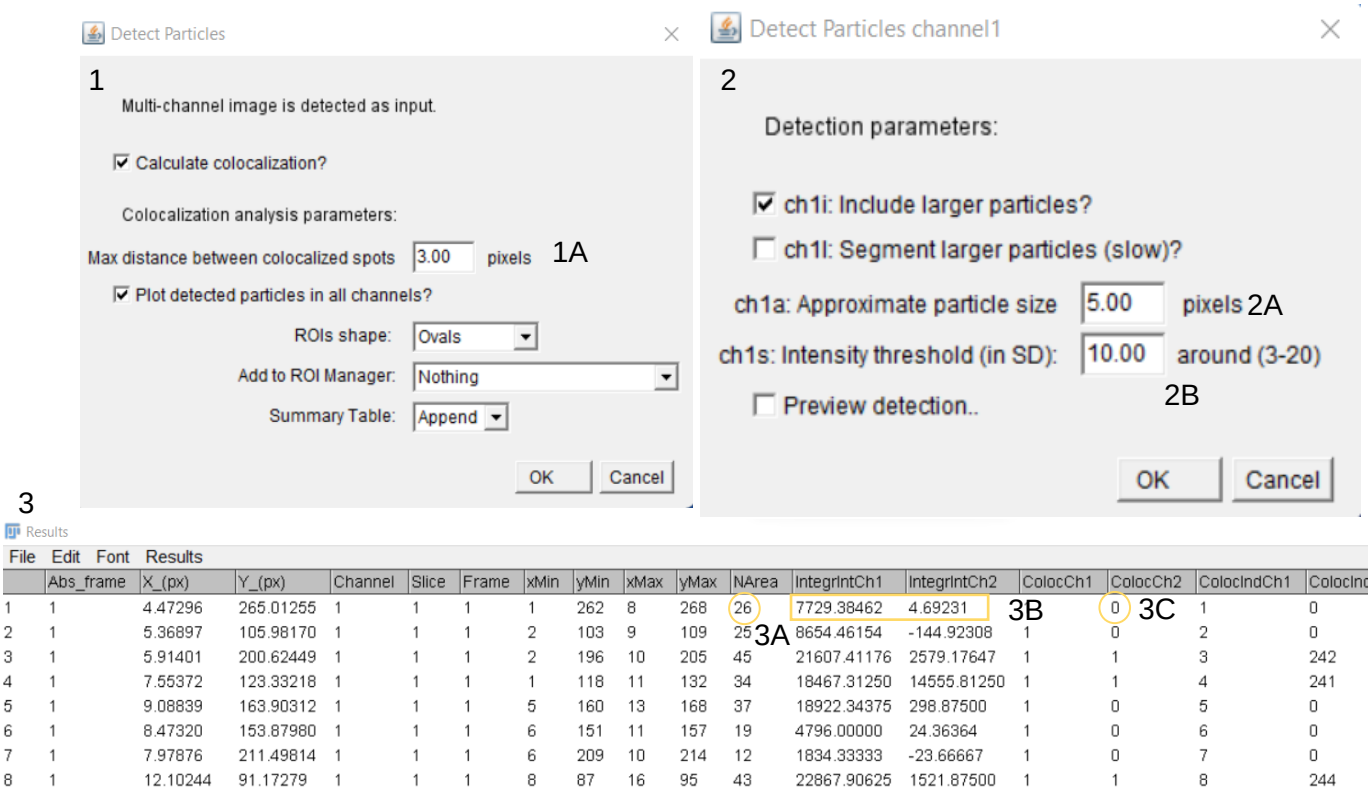

	Abs_frame	X_(px)	Y_(px)	Channel	Slice	Frame	xMin	yMin	xMax	yMax	NArea	IntegrIntCh1	IntegrIntCh2	ColocCh1	ColocCh2	ColocIndCh1	ColocIndCh2	Index
1	1	4.47296	265.01255	1	1	1	1	262	8	268	26	7729.38462	4.69231	1	0	1	0	1
2	1	5.36897	105.98170	1	1	1	2	103	9	109	25	8654.46154	-144.92308	1	0	2	0	2
3	1	5.91401	200.62449	1	1	1	2	196	10	205	45	21607.41176	2579.17647	1	1	3	242	3
4	1	7.55372	123.33218	1	1	1	1	118	11	132	34	18467.31250	14555.81250	1	1	4	241	4
5	1	9.08839	163.90312	1	1	1	5	160	13	168	37	18922.34375	298.87500	1	0	5	0	5
6	1	8.47320	153.87980	1	1	1	6	151	11	157	19	4796.00000	24.36364	1	0	6	0	6
7	1	7.97876	211.49814	1	1	1	6	209	10	214	12	1834.33333	-23.66667	1	0	7	0	7
8	1	12.10244	91.17279	1	1	1	8	87	16	95	43	22867.90625	1521.87500	1	1	8	244	8

Figure 2.1 – Fiji Comdet plugin Analysis of colocalization and puncta intensity

(**A**) – Comdet first parameters including the shape of the objects and the max distance considered for colocalization (**1A)**

(**B)** – Comdet detection parameters that allow to detect of the puncta of interest, by choosing the approximate particle size (**2A**) and intensity threshold (**2B**).

(**C**) – Comdet results with the information of the size of each puncta identified (**3A**), the intensity (**3B**) and whether colocalizes (1) or not (0) (**3C**).

Qualitative analysis

We used Fiji to analyze the presence of APP and F-actin on enlarged endosomes (Figure 3.7D and 3.7E). First, we outlined the outer membrane of endosomes using the "Polygon selection" tool on the Rab5QL channel. Then, by observation, we identified the outlined endosomes as positive or negative for APP bright puncta often found in the endosomal lumen and F-actin bright puncta on the outer aspect endosomal membrane.

III.7 STATISTICS

Graphs were generated using GraphPad Prism 7. Data are shown as mean ± standard error of the mean (SEM). Statistical analysis was conducted with at least three independent experiments. One one-way ANOVA with Tukey's multiple comparisons test was used for parametric unpaired data. For non-parametric unpaired data, the Kruskal-Wallis test was used. Statistical significance was placed at $p<0.05$.

IV. PREVIOUS RESULTS

Previously, Cláudia Almeida's lab showed that CD2AP controls the endocytic trafficking of APP during early endosome maturation. CD2AP knockdown reduced the sorting within endosomes from the limiting membrane to the lumen, step required for efficient degradation at the lysosome. The APP accumulation on the endosomal membrane likely facilitates APP amyloidogenic processing since Aβ production increased. The question of how CD2AP controls APP trafficking is being investigated.

Since CD2AP is an actin-binding protein and actin can control endocytic trafficking, we hypothesized that CD2AP might control APP endocytic sorting via F-actin.

First, to determine if F-actin was present in early endosomes, F-actin was labelled with Phalloidin, an actin probe. Its colocalization with early endosome antigen 1 (EEA1), an early endosome marker in comparison with late-endosomes/lysosomes, identified with Lysosome-associated membrane glycoprotein 1 (Lamp1) and Mannose 6-phosphate receptor (MPR), enriched in the trans-Golgi network (TGN) was quantified in neuronal cells (n2a). Early endosomes showed a clear enrichment of F-actin foci with ~35% of the EEA1 colocalizing with F-actin, more than late endosomes/lysosomes and TGN (20%) (Figure 1A).

Second, endogenous CD2AP was stained to determine its association with early endosomes and F-actin. A pool of CD2AP (20%) colocalized with early endosomes (EEA1 and Rab5) and F-actin (Figure 1B).

Third, whether the absence of CD2AP could result in defects in F-actin association with early endosomes was tested. N2A cells transfected with siRNA specific against CD2AP (siCD2AP) and a non-targeting siRNA (siControl) were stained for F-actin and EEA1. Interestingly, the knockdown of CD2AP affected the F-actin at the perinuclear region of N2a cells, a region enriched in early endosomes, as shown by the nearly 50% decrease of the fraction of cellular F-actin in the perinuclear region (perinuclear F-actin).

Fourth, by using confocal microscopy, it was found that CD2AP reduced the number of early endosomes positive for F-actin, the intensity of F-actin associated with early endosomes (endosomal F-actin), the number of F-actin foci in the perinuclear region as well as the number of early endosomes.

Altogether, these unpublished results suggest that the absence of CD2AP affects the F-actin associated with early endosomes in the perinuclear region, which can affect the endocytic traffic.

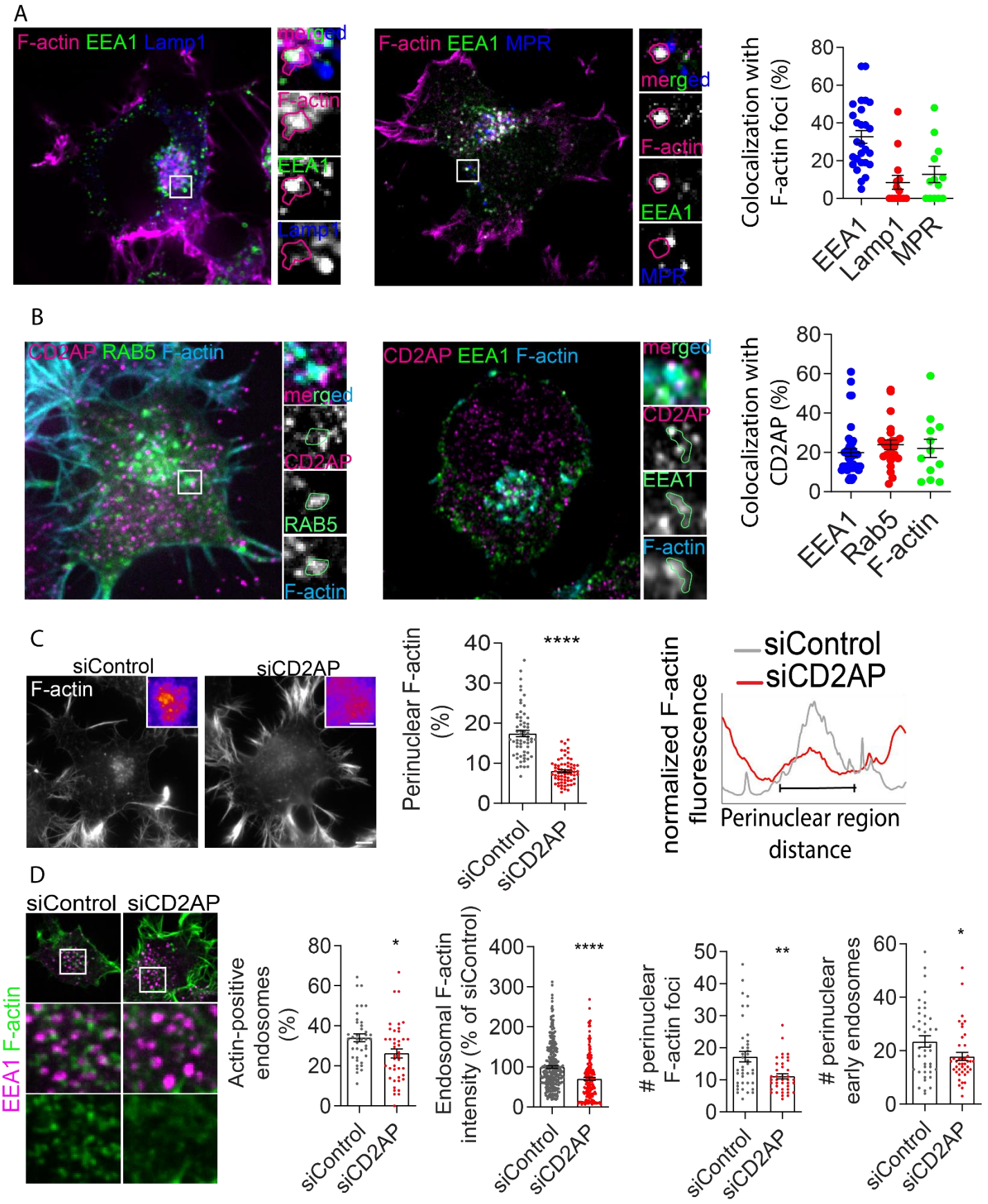

Figure 3.1 Previous results obtained on F-actin impact on endosomes.

(A) Colocalization of F-actin foci with early endosomes (EEA1), late endosomes and lysosomes (LAMP1) and the trans-Golgi network (MPR). (n=1; mean ± SEM)

(B) Colocalization of endogenous CD2AP with early endosomes (EEA1 and Rab5) and F-actin (n=1; mean ± SEM)

(C) Impact of CD2AP downregulation on perinuclear F-actin

(n = 5; ****P < 0.0005 vs. siControl, t-test; mean ± SEM)

(D) Impact of CD2AP downregulation on actin-positive endosomes, endosomal F-actin, number of perinuclear F-actin foci and number of perinuclear early endosomes.

(n = 5; ****P < 0.0005 vs. siControl, t-test; mean ± SEM)

V. RESULTS

V.1 CD2AP RESCUES THE PERINUCLEAR F-ACTIN REDUCTION INDUCED BY CD2AP KNOCKDOWN

Since, in previous work, we observed that treatment with siRNA against CD2AP (siCD2AP) decreases the perinuclear F-actin, we evaluated if re-expression of CD2AP rescues the perinuclear F-actin to rule out non-specific targets of the siCD2AP. Moreover, we also investigated if a mutation in CD2AP associated with late-onset AD (K633R) affected the CD2AP function in maintaining the perinuclear F-actin.

To rescue CD2AP, we downregulated endogenous CD2AP expression using siCD2AP, re-introduced wild-type CD2AP or mutant CD2AP (K633R), and assessed the % of F-actin in the perinuclear region (perinuclear F-actin) and the intensity of the perinuclear F-actin foci (endosomal F-actin) (Figure 3.2). We used a non-targeting siRNA as control (siControl) and a rescue control by reexpressing only GFP (empty plasmid). F-actin was labelled using fluorescent phalloidin.

We observed that F-actin in siControl cells distributes between two main pools, the peripheral cortical F-actin and the perinuclear endosomal F-actin. In siCD2AP cells expressing GFP, we noted a change in F-actin distribution, being less prominent in the perinuclear region. These observations were consistent with previous findings in siCD2AP cells (Figure 3.2A).

Quantification revealed nearly 20% of F-actin in the perinuclear region in siControl cells, while in siCD2AP cells expressing GFP, the perinuclear F- actin decreased to 10%, recapitulating previous results. CD2AP wild-type re-expression in cells knockdown for CD2AP rescued the perinuclear F-actin, no longer different from siControl. In one pilot experiment, we observed that the mutant CD2AP (K633R) did not rescue perinuclear actin (Figure 3.2B).

To assess the intensity of each F-actin foci in the perinuclear region, we identified the region of interest (ROI) in the perinuclear region of the cell by outlining it using the circular region tool and used the Comdet plugin to segment and measure the intensity of each F-actin foci, with Fiji. CD2AP depletion results in a 50% decrease in puncta intensity compared to the siControl, being rescued by the WT CD2AP but not by mutant CD2AP re-expression (Figure 3.2C).

We also noticed morphological changes in the cell cortex. While wild-type cells showed few F-actin positive protrusions, likely filopodia, the lack of CD2AP changed this phenotype, increasing the number of filopodia-like protrusions. This may indicate a secondary site of action for CD2AP since CD2AP has been reported to function at the cell cortex in non-neuronal cells (Jianping Zhao et al., 2013).

Altogether, these results indicate that CD2AP specifically controls the perinuclear F-actin. In future experiments, it will be important to confirm if the LOAD mutation (K633R) causes CD2AP loss of function.

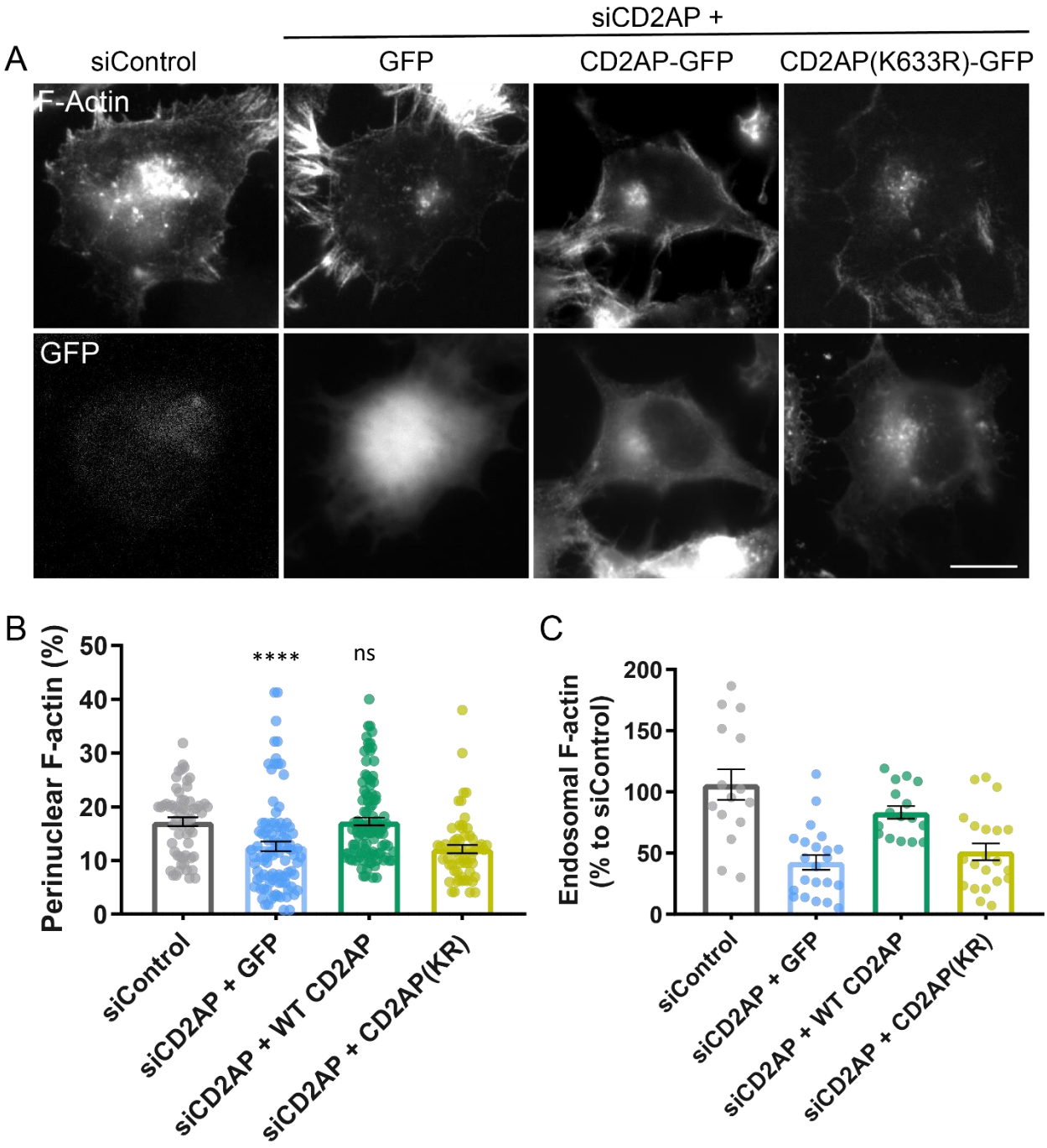

Figure 3.2 – CD2AP knockdown reduces specifically perinuclear F-actin.
(**A**) Representative images of N2a cells treated with non-targeting siRNA (siControl), or siRNA against CD2AP (siCD2AP) and expressing GFP, CD2AP-GFP or CD2AP(K633R)-GFP and stained for F-actin with phalloidin (Top panels). GFP fluorescence (Bottom panels). Scale bar, 10 µm.
(**B**) Quantification of the percentage of perinuclear F-actin fluorescence relative to whole cell total F-actin fluorescence.
(n = 3 for siControl, siCD2AP + GFP and siCD2AP + WT CD2AP; N = 67-107 cells; ****P < 0.0005 vs. siControl, t-test; mean ± SEM)
(**C**) Quantification of mean intensity of F-actin puncta in the perinuclear region, presented as percentage of siControl cells. (n = 1, N = 15-23 cells; mean ± SEM)

V.2 ARPC1A RESCUES THE PERINUCLEAR F-ACTIN REDUCTION INDUCED BY ARPC1A KNOCKDOWN

The main mechanism of F-actin polymerization on endosomes is Arp 2/3 complex-mediated, which regulates different cellular processes with different nucleator-promoting factors and actin-binding proteins. Furthermore, the Arp 2/3 consists of several subunits, some with alternative isoforms, allowing for the formation of diverse Arp2/3 complexes, suggesting differences in their location and type of actin polymerized (Abella et al., 2016; Jay et al., 2000).

We hypothesized whether an Arp2/3 subcomplex could be specifically involved in the polymerization of perinuclear endosomal F-actin. If that is the case, then its knockdown should replicate the CD2AP loss of function phenotype. Indeed, in previous work in the lab, it was observed that ARPC1A but not ARPC1B caused depletion of the perinuclear endosomal F-actin, similarly to CD2AP knockdown. To confirm the specificity of the siRNA sequences used to knockdown ARPC1A, we performed a rescue experiment by reexpressing ARPC1A. We also confirmed the specificity of a siRNA against the ARPC2 subunit, fundamental for the activity of the Arp 2/3 complex, used to knockdown all Arp2/3 subcomplexes (Figure 3.3).

We observed that the three different sequences for the knockdown of ARPC1A led to a decrease in the intensity of perinuclear F-actin-like CD2AP knockdown. We also noted an increase in the formation of filopodia-like structures with a bright F-actin signal. Re-expressing ARPC1A rescued the F-actin signal in the perinuclear region similarly in cells treated with the three siRNA sequences against ARPC1A. Lastly, the absence of the ARPC2 subunit caused a dramatic decrease in the whole cell F-actin intensity, most cells were devoid of any cell protrusion, and f-actin stress fibres were often present. These effects were rescued by re-expressing ARPC2 (Figure 3.3B)

Despite the diffuse cytosolic signal, we also observed that the ARPC1A-GFP often colocalized with F-actin foci in the perinuclear region (Figure 3.3A).

These observations were then confirmed by quantifying the distribution of perinuclear F-actin. Regarding the siControl cells, we observed that F-actin distribution to the perinuclear region (18%) was consistent with the previous experiment. In cells knockdown for ARPC1A, we observed a similar decrease of 10% in perinuclear F-actin across all the different siRNA sequences used (Figure 3.3B). Moreover, the intensity of endosomal F-actin decreased by 25% to 47% in siARPC1A cells relative to siControl cells (Figure 3.3C). The knockdown of ARPC2 caused the biggest impact on F-actin, which was overall decreased. Nevertheless, we quantified a decrease of 10% in the percentage of F-actin in the perinuclear region and a 35% decrease in the endosomal F-actin in siARPC2 cells. Once we reintroduced the corresponding Arp 2/3 subunit, we saw an overall recovery of the perinuclear actin across all conditions. All siARPC1A sequences increase the perinuclear actin to levels similar

to the control (14 to 16 %). The endosomal F-actin was also rescued, increasing above control, suggesting an effect due to the subunit's overexpression. Interestingly, while the knocked down of the subunit ARPC2 resulted in the most significant decrease in F-actin distribution and intensity, once we re-expressed ARPC2, the levels of perinuclear actin increased from 10% to 16%, and the endosomal F-actin increased from 35% to 168% of the control levels.

Altogether, these results indicate a favoured polymerization region for the ARPC1A-containing complex, as shown by the decrease in perinuclear and endosomal F-actin. These results reflect the same defects in actin polymerization as the loss of function in CD2AP, suggesting, thus, a possible association with endosomes.

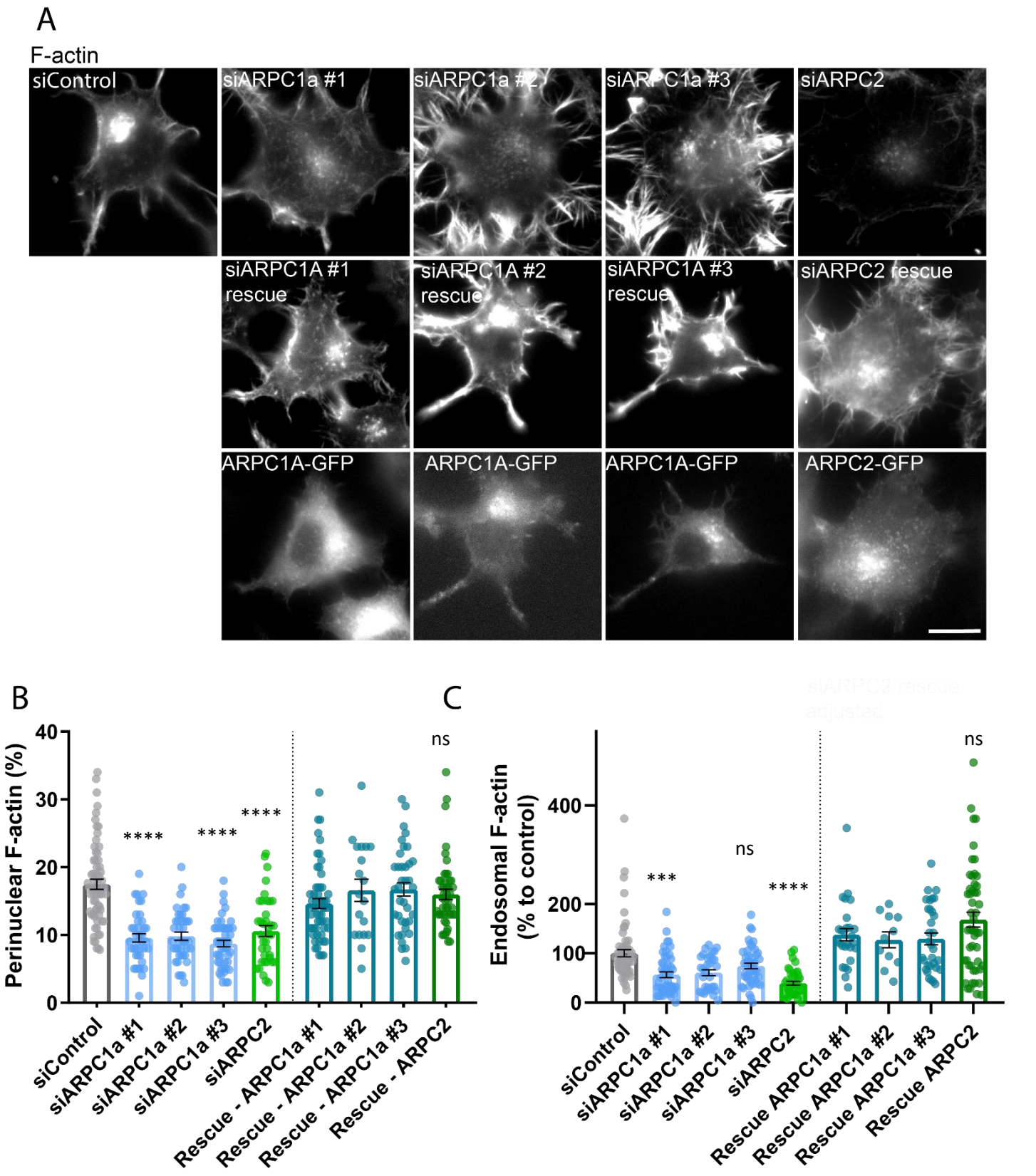

Figure 3.3 – ARPC1A knockdown reduces specifically perinuclear F-actin.

(**A**) F-actin labelled with phalloidin in N2a cells treated with non-targeting siRNA (siControl), or siRNA against ARPC1A (#1, #2 and #3) (siARPC1A) and ARPC2 (siARPC2) expressing ARPC1A-GFP or ARPC2-GFP respectively. GFP fluorescence (Bottom panels). Scale bar, 10 µm.

(**B**) Quantification of the percentage of perinuclear F-actin fluorescence relative to whole cell total F-actin fluorescence. (n = 4 for siControl, n= 3 for siARPC1A #1, #3, siARPC2 and Rescue of ARPC2, N = 49-91 cells; ****P < 0.0005 vs. siControl, t-test; mean ± SEM)

(**C**) Quantification of mean intensity of F-actin puncta in the perinuclear region, presented as percentage of siControl cells. (n= 4 for siControl, n = 3 for siARPC1A #1, #3, siARPC2 and Rescue of ARPC2, N = 46-63 cells; ****P < 0.0005 vs. siControl, t-test; mean ± SEM)

V.3 ARPC1A-CONTAINING ARP 2/3 COMPLEX REGULATES CD2AP EXPRESSION AND LOCALIZATION

CD2AP has been shown to function as a scaffold bridging F-actin to other proteins. We decided to ask if interfering with endosomal F-actin via ARPC1A knockdown affected CD2AP expression and localization to the perinuclear actin.

We knocked down the ARPC1A to decrease endosomal F-actin and ARPC2 to decrease F-actin and labelled endogenous CD2AP by immunofluorescence. To confirm any non-specific effect of the siRNA treatments, we re-introduced the Arp 2/3 subunits through plasmid transfection as in the previous experiments. The total levels of CD2AP and perinuclear CD2AP.

CD2AP appeared in a punctate pattern throughout the cytoplasm, with a part concentrated in the perinuclear region (15%). Upon siARPC1A and C2, we observed as a general reduction in CD2AP intensity (Figure 3.4A).

The reexpression of the ARPC1A and ARPC2 subunits restored and even increased the total levels of CD2AP above the siControl levels. Quantifying cellular CD2AP levels supports that ARPC1A depletion tends to reduce the levels of CD2AP (Figure 3.4B), especially in the perinuclear region (Figure 3.4C). With the re-expression of ARPC1A and ARPC2, the CD2AP levels in the perinuclear region increased to the control level.

This data indicates a role for ARPC1A isoform in endosomal F-actin and the CD2AP perinuclear localization.

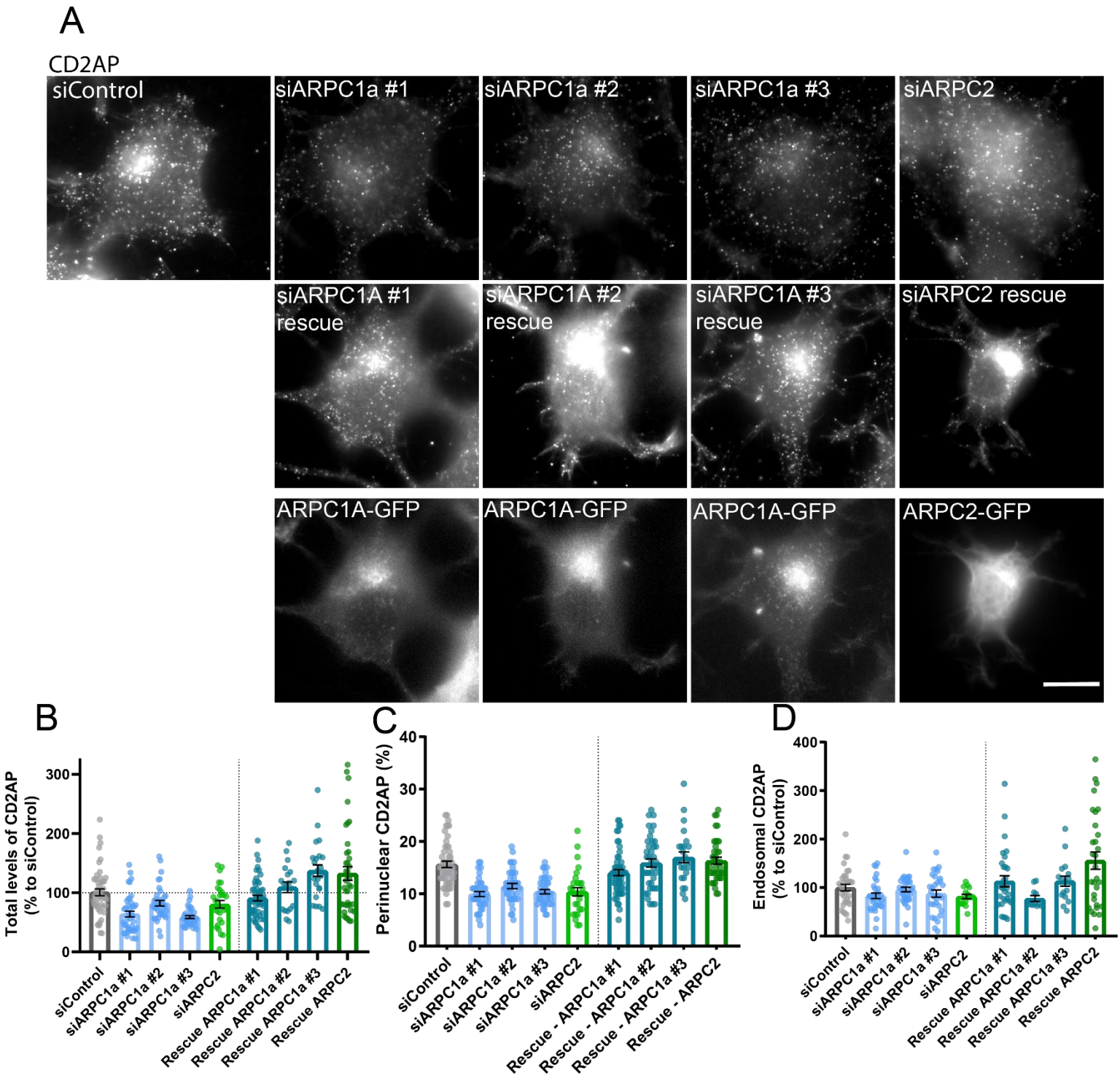

Figure 3.4 - ARPC1A isoform modulates CD2AP expression and localization

A) CD2AP immunofluorescence in N2A cells treated with non-targeting siRNA (siControl), or siRNA against ARPC1A (#1, #2 and #3) (siARPC1A) and ARPC2 (siARPC2) expressing ARPC1A-GFP or ARPC2-GFP respectively. GFP fluorescence (Bottom panels). Scale bar, 10 µm.

(**B)** Quantification of the percentage of total levels of CD2AP fluorescence, presented as percentage of siControl cells. (n = 2, N = 20-52 cells; mean ± SEM)

(**C**) Quantification of the percentage of perinuclear CD2AP fluorescence relative to the whole cell total CD2AP fluorescence (n = 2, N = 25-55 cells; mean ± SEM)

(**D**) Quantification of mean intensity of F-actin puncta in the perinuclear region, presented as percentage of siControl cells. (n = 2, N = 11-32 cells; mean ± SEM)

V.4 ARPC1A CONTAINING COMPLEX PROMOTES CD2AP ENRICHMENT AT ENDOSOMES

ARPC1A knockdown was shown to affect the perinuclear F-actin and CD2AP, but how the ARPC1A associates with F-actin and CD2AP puncta on endosomes is not known. Thus, we decided to characterize the ARPC1A localization in endosomes, further comparing it with ARPC1B, the alternative isoform.

To explore the distribution of the ARPC1 isoforms on endosomes, we overexpressed ARPC1A-GFP or ARPC1B-GFP together with Rab5(Q79L)-Myc (Rab5QL), a constitutively active form of the GTPase Rab5, enabling the enlargement of early endosomes, in N2a cells. Then, we immunolabelled for CD2AP or F-actin and assessed the presence of ARPC1A and ARPC1B in enlarged RAB5QL endosomes and the enrichment of CD2AP and F-actin when colocalized with the ARPC1 isoforms (Figure 3.5 C, I, G).

As expected, we observed the formation of enlarged endosomes marked by the Rab5QL-myc plasmid (Figure 3.5). Unexpectedly, both ARPC1A-GFP (Figure 3.5A) and ARPC1B-GFP (Figure 3.5B) frequently decorated the membrane of Rab5QL endosomes. Furthermore, upon ARPC1A overexpression, we observed that some enlarged endosomes had attached smaller RAB5QL vesicles that could be fusing in or budding out, which had ARPC1A with CD2AP foci localized at their base (Figure 3.5A1 and 3.5A2).

To analyse the enrichment of CD2AP and F-actin when colocalized with the ARPC1 isoforms, we used the Fiji plugin “Comdet” to detect whether the CD2AP puncta colocalized or not with ARPC1A/B-GFP at the endosomal membrane. Then, we assessed the CD2AP intensity when colocalized with each ARPC1 isoform relative to the intensity of CD2AP alone. We observed that CD2AP intensity, when colocalized with ARPC1A, increased by 180%. In contrast, the CD2AP intensity, when colocalized with ARPC1B, did not increase relative to CD2AP alone. (Figure 3.5C). Additionally, CD2AP colocalized more with ARPC1A than ARPC1B on the endosomal membrane (Figure 3.5D). These results suggest CD2AP is more associated with the Arp2/3 complex containing the ARPC1A than the ARPC1B subunit.

We observed that endosomal F-actin foci intensity increased (300%) when ARPC1A and ARPC1B colocalized relative to F-actin alone (Figure 3.5G). The colocalization of endosomal F-actin with ARPC1 isoforms was also the same (Figure 3.5H).

In sum, by studying the two ARPC1 isoforms parallelly, we observe a higher capability of CD2AP to associate with the isoform ARPC1A. Furthermore, we identified a new phenotype induced by the ARPC1A overexpression characterized by an endosomal budding enriched in ARPC1A with CD2AP often localized at the base. Altogether this data reinforces a synergistic role of ARPC1A and CD2AP in the control of F-actin at endosomes.

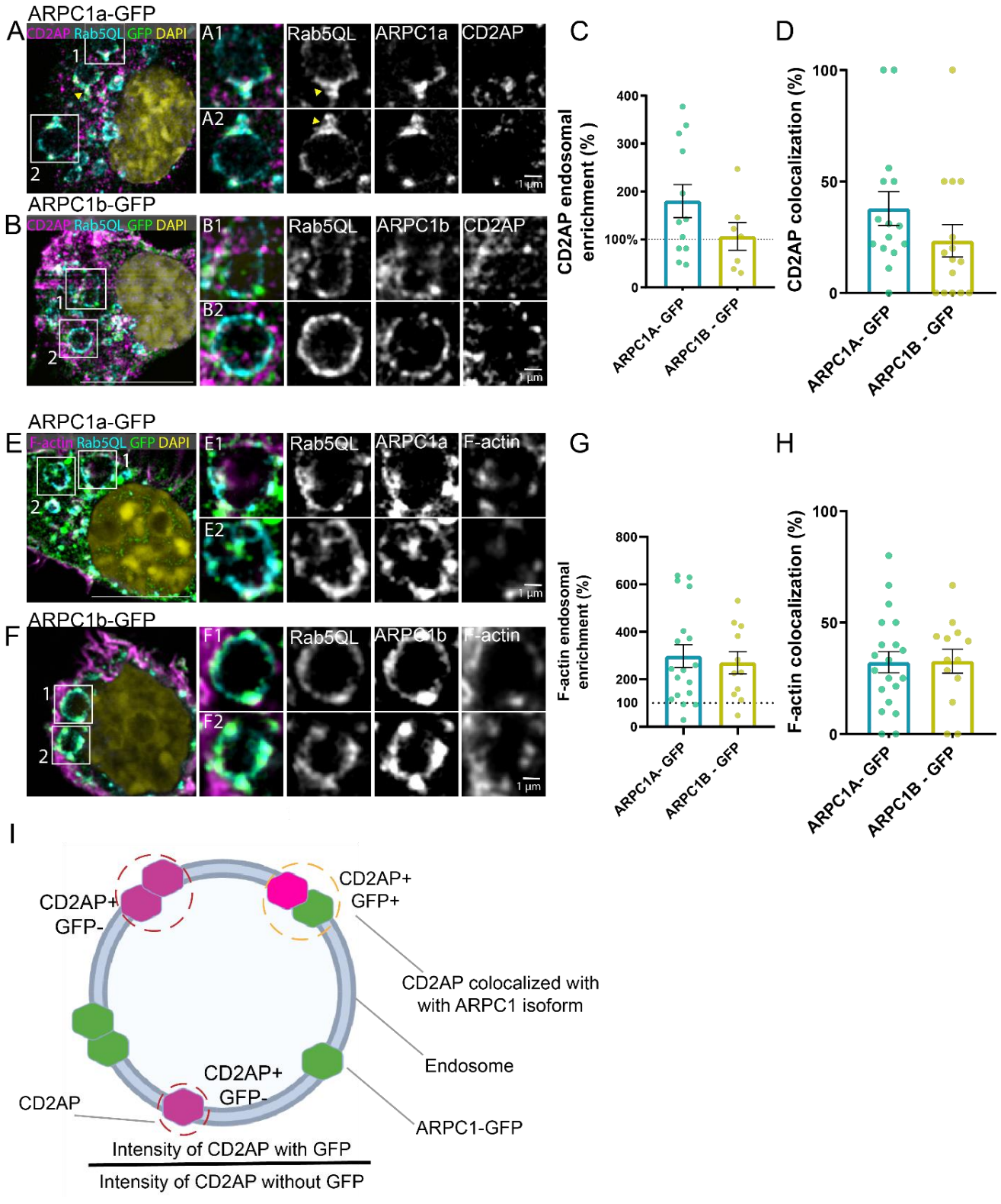

Figure 3.5 – ARPC1 isoforms differentially regulate early endosome F-Actin polymerization and CD2AP association.
(A, B) CD2AP (magenta) and immunofluorescence in N2a cells expressing Rab5QL-myc (Cyan) with ARPC1A-GFP (Green) (**A**) or ARPC1B-GFP (Green) (**B**). DAPI labelling of nucleus (Yellow). Scale bar, 10 µm. White squares indicate a Rab5QL-positive endosome magnified on the right. **A1, A2** and **B1, B2** Merged CD2AP (magenta) and ARPC1A/B (Green) distribution within enlarged Rab5QL-GFP endosomes (cyan). Each labelling is also shown individually in grey. Scale bar, 1 µm.
(**C**) Quantification of the percentage of CD2AP endosomal enrichment when colocalized with ARPC1A or ARPC1B.
(n = 1, N = 8-12 endosomes; mean ± SEM)
(**D**) Colocalization of CD2AP on the endosomal membrane with ARPC1A-GFP or ARPC1B-GFP
(n = 1, N = 14-15 endosomes; mean ± SEM)

(**E, F**) Representative images of N2a cells expressing Rab5QL-myc with ARPC1A-GFP (**A**) or ARPC1B-GFP (**B**). Cells stained for F-actin (magenta), Rab5QL-myc (Cyan). GFP fluorescence. Scale bar, 10 µm.
E1, E2 and **E1,E2 -** Indicate intersections from amplified endosomes including the merge staining and also the individual labelling in black and white. Intersections were obtained from panel **E** and **F** correspondingly.
(**G)** Quantification of the percentage of F-actin endosomal enrichment when colocalized with ARPC1A or ARPC1B.
(n = 1, N = 11-18 endosomes; mean ± SEM)
(**H**) Colocalization of F-actin on the endosomal membrane with ARPC1A-GFP or ARPC1B-GFP
(n = 1, N = 13-20 endosomes; mean ± SEM)
(**G**) Representation of method of quantification for CD2AP and F-actin Endosomal Enrichment (**C,G**)

V.5 ARP 2/3 SUBUNITS IMPACT ON APP ENDOCYTIC TRAFFICKING

V.5.1 Arp 2/3 subunits impact early endosomes

In a lab publication, CD2AP knockdown was described to affect APP sorting at early endosomes. Thus, we next investigated the impact of the loss of function of the ARPC1 isoforms and ARPC2 on APP localization in early endosomes, comparing it to CD2AP loss of function. For that, we transfected N2a cells against the target proteins for 72h and labelled EEA1, F-actin, and APP, with the anti-APP (Y188) that recognizes the C-terminal motif of APP (Figure 3.6A). We then measured the perinuclear F-actin to confirm the knockdown efficacy of the siArp 2/3 subunits and CD2AP. We quantified the intensity of the APP present at EEA1+ endosomes. As well as the EEA1+ early endosomes distribution to the perinuclear region, intensity, and size, and using Fiji and its Comdet plugin

We then quantified the EEA1 intensity, size, and APP-Y188 intensity at each EEA1 vesicle. In preliminary experiments, we observed the previously reported cell morphology labelled by F-actin, where siARPC1A and siCD2AP increased the number of filopodia-like structures and siARPC2 decreased the overall F-actin. The morphology of cells treated with siARPC1B was similar to siControl. We also observed a decrease in EEA1 and APP labelling at the perinuclear region for the siARPC1A and siARPC2 (Figure 3.6A). At higher magnification, APP did not seem to colocalize greatly with EEA1 vesicular staining, which suggested other endocytic compartments of APP localization (Figure 3.6A, magnified regions).

Quantification revealed that 25% of the EEA1+ signal was located in the perinuclear region. The knockdown of ARPC1A, ARPC2, and CD2AP showed a tendency to decrease the perinuclear EEA1, which remained unaltered upon ARPC1B knockdown (Figure 3.6B).

Similarly, siARPC1A, siARPC2, and siCD2AP treatment reduced the EEA1 intensity per vesicle below 60%, with siARPC1A reaching 46%, while the siARPC1B showed no defects compared to the control (Figure 3.6C).

The size of EEA1 tended to decrease in siARPC1A, siARPC2 and siCD2AP treated cells, while siARPC1B treatment led to no defects (Figure 3.6D). Lastly, the APP intensity at EEA1 puncta reduced from 66% in the ARPC2 to 51% in the ARPC1A (Figure 3.6E).

So far, our data shows that the ARPC1A loss of function affects early endosomes, decreasing its perinuclear distribution, size, and the intensity of APP within $EEA1^{+}$ endosomes similarly to CD2AP, while the absence of ARPC1B does not seem to have an impact on endosomes.

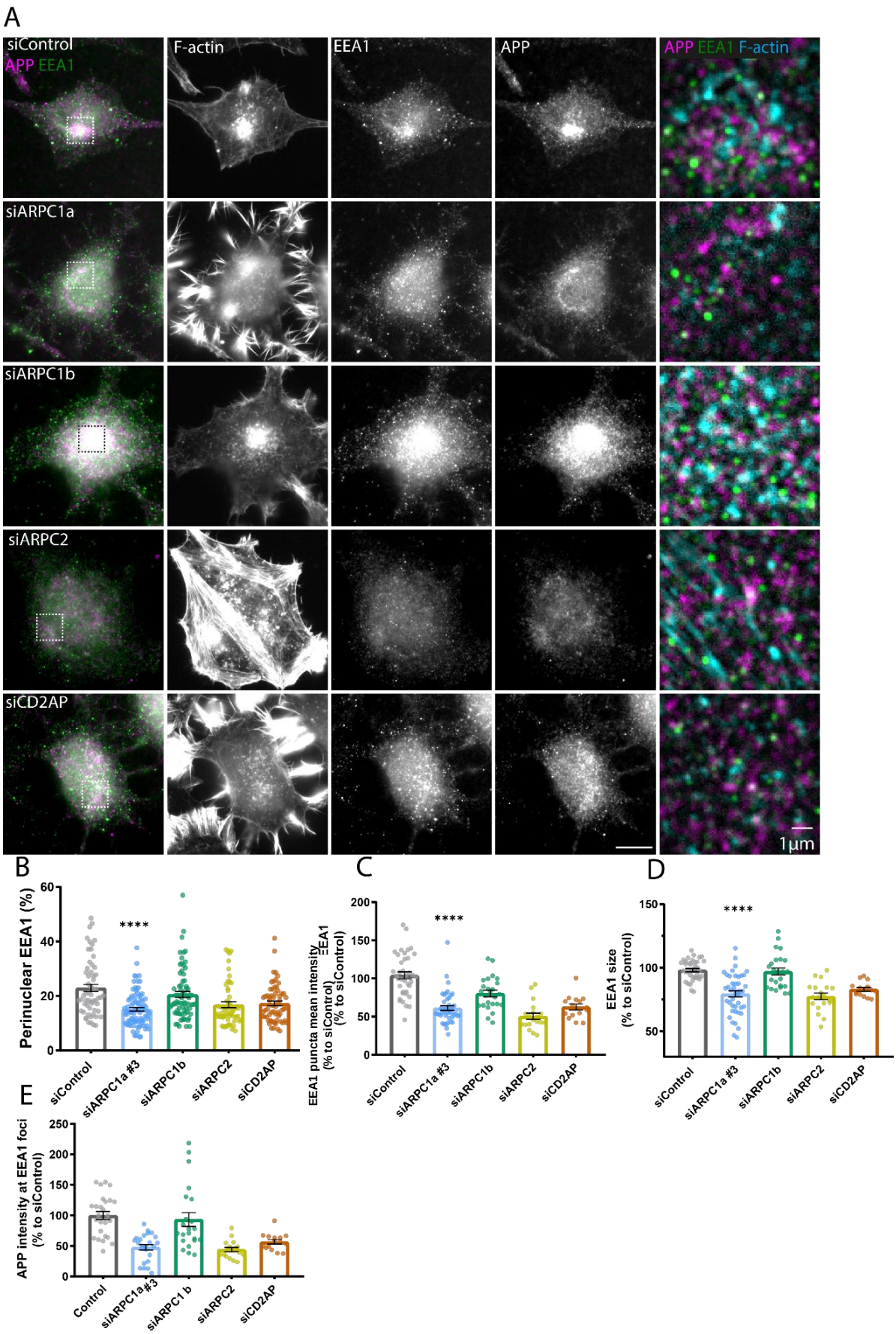

Figure 3.6 - ARPC1A isoform affects early endosomes at the perinuclear region

A) Representative images of N2a cells treated with non-targeting siRNA (siControl), or siRNA against ARPC1A (#3) (siARPC1A), ARPC1B (siARPC1B), ARPC2 (siARPC2) and CD2AP (siCD2AP). Cells stained for APP (magenta), EEA1 (green) and F-actin (cyan). Right panel represents a magnification from the perinuclear region of the respective condition.

(**B)** Quantification of the percentage of perinuclear EEA1 fluorescence relative to the whole cell total EEA1 fluorescence

(n = 3 for siControl and siARPC1A, N = 46-77 cells; ****P < 0.0005 vs. siControl, t-test; mean ± SEM)

(**C**) Quantification of mean intensity of EEA1 puncta in the perinuclear region, presented as percentage of siControl cells.

(**D**) Quantification of the percentage of EEA1 size, presented as percentage of siControl cells.
(n = 3 for siControl and siARPC1A, N = 19-38 cells; ****P < 0.0005 vs. siControl, t-test; mean ± SEM)
(**E**) Quantification of intensity of APP fluorescence at EEA1 puncta in the perinuclear region, presented as percentage of siControl cells. (n = 2, N = 15-26 cells; mean ± SEM)

V.5.2 Arp 2/3 subunits impact APP endosomal distribution and endosomal F-actin

The previous experiments indicate that ARPC1A, but not ARPC1B, is present on endosomes and required for perinuclear F-actin. CD2AP was also shown to colocalize more with ARPC1A than ARPC1B on endosomes. Furthermore, we also observed that ARPC1A depletion might cause defects in early endosomes and APP in early endosomes. Now, we wanted to assess the function of ARPC1 isoforms in APP endosomal sorting. Taking into consideration that we have previously demonstrated that CD2AP loss of function affects APP endosomal sorting, with an increased APP on the endosomal membrane (Ubelmann et al., 2017), we hypothesized that ARPC1A loss of function might cause a similar defect. We also hypothesized that it decreases the endosomal F-actin.

To assess that, we knocked down ARPC1A, ARPC1B, ARPC2, and CD2AP for 72h, and 24h before fixing, we transfected the cells with Rab5QL-myc to enlarge endosomes and distinguish between the endosomal membrane, the site of APP processing, and the lumen, containing ILVs that direct APP for degradation. Then, we immunolabelled with APP-Y188, anti-myc, and F-actin. All the conditions were compared to a siControl condition.

In preliminary experiments, we observed that, as previously, the overexpression of the mutant GTPase, Rab5QL, induced the formation of large endosomes. In the siControl and siARPC2 cells, APP-Y188 was detected in the lumen of many enlarged endosomes (Figure 3.7A). In the siARPC1A and siARPC1B cells, we observed fewer endosomes containing APP.

By quantifying the intensity of APP per endosome, we observed that it decreased upon the knockdown of ARPC1B and CD2AP but not upon the knockdown of ARPC1A and ARPC2 (Figure 3.7B).

As for the distribution of APP on the endosomal membrane, we observed a slight increase of APP, with siARPC1A showing only a 6% increase over the siControl condition (Figure 3.7C). We also found the % of endosomes containing APP reduced upon siARPC1A, siARPC1B, and siCD2AP but strangely not siARPC2 treatment (Figure 3.7D). Furthermore, we qualitatively counted the endosomes containing F-actin in the percentage of the total number of endosomes per each condition. In siControl cells, we observed that 78% of the endosomes had F-actin patches, which tended to decrease with the knockdown of ARPC1A, ARPC2, and CD2AP to 51, 55, and 58%, respectively, but not with the knockdown of ARPC1B (Figure 3.7E).

These results suggest that the ARPC1A isoform might regulate F-actin polymerization on endosomes. Moreover, the decrease observed in the endosomes containing APP supports the previous report by Ubelmann *et al.,* where APP was reduced in EEA1-positive early endosomes of CD2AP-depleted neurons.

However, by inhibiting BACE1 with DAPT and thus, hindering APP processing, Ubelmann et al. observed a fourfold increase in APP on early endosomes of CD2AP-depleted dendrites. Moreover, the APP on the endosomal membrane also increased from 40% to 60% by inhibiting BACE1. In the future, we aim to repeat these experiments using DAPT to inhibit APP processing and allow us to assess the effects of the ARPC1A on APP endosomal sorting.

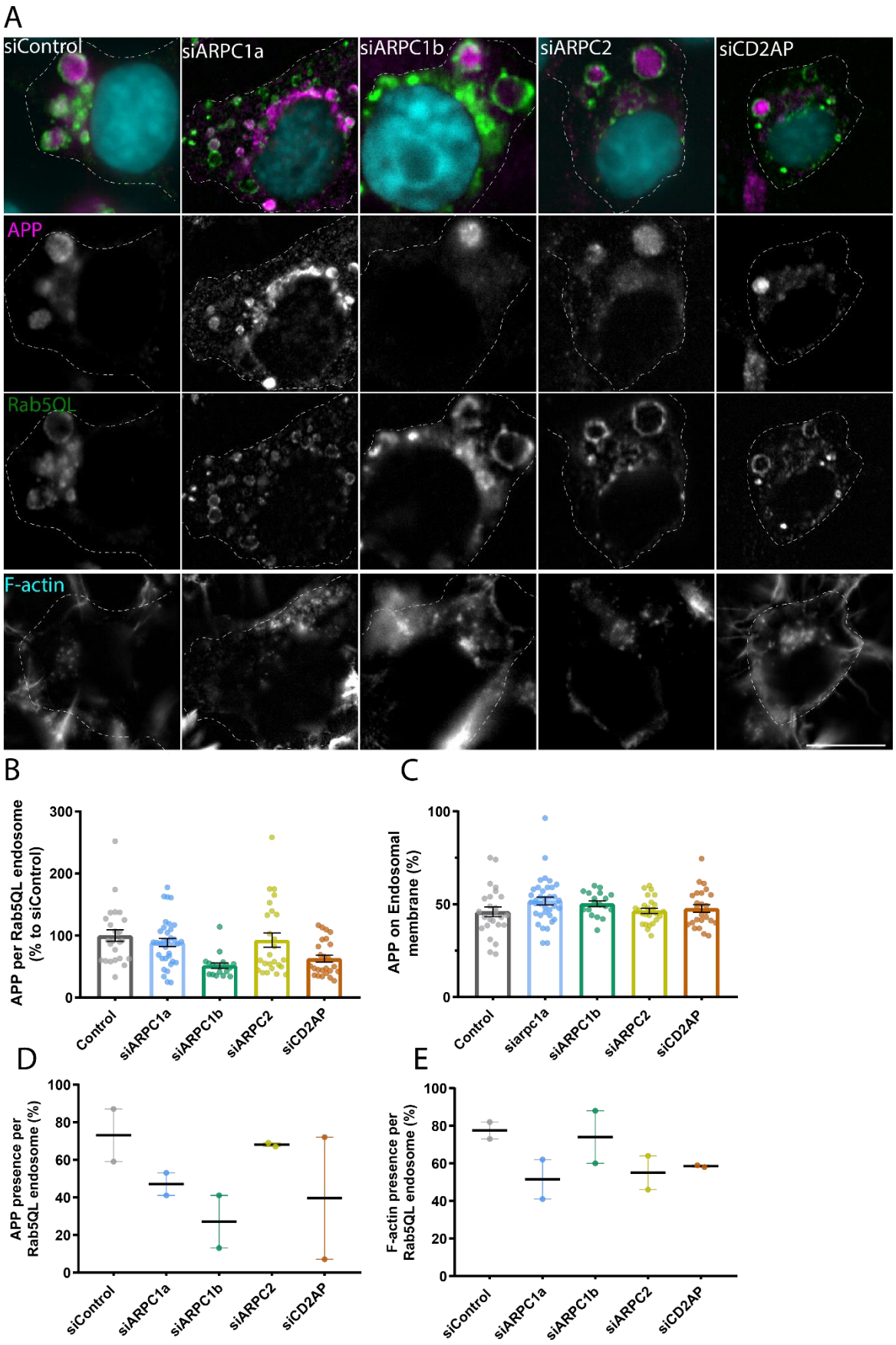

Figure 3.7 – Effect of ARP subunits knockdown on APP endosomal distribution.

A) Representative images of N2a cells treated with non-targeting siRNA (siControl), or siRNA against ARPC1A (#3) (siARPC1A), ARPC1B (siARPC1B), ARPC2 (siARPC2) and CD2AP (siCD2AP), expressing Rab5QL-myc. Cells stained for APP-Y188 (magenta), Rab5QL-myc (green) and F-actin (black and white)

(**B)** Quantification of the percentage of APP fluorescence per Rab5QL endosome, presented as percentage of siControl cells. (n = 2, N = 18-34 cells; mean ± SEM)

(**C**) Quantification of the percentage of APP fraction present on the Rab5QL endosomal membrane relative to the APP intensity of the whole endosome. (n = 2, N = 18-36 cells; mean ± SEM)

(D,**E**) Qualitative analysis of the percentage of endosomes containing APP (**D**) or F-actin (**E**) relative to the total number of endosomes. Presented as two independent experiments (n = 2, N = 27-32 cells; mean ± SEM)

V.5.3 ARPC1A isoform impact on APP degradation

Next, we assessed whether ARPC1A could lead to APP endocytic trafficking defects. CD2AP was previously shown to regulate the degradation of APP as the loss of function led to a significant decrease in surface APP degradation after a chase of 60 minutes (Ubelmann, 2017). We decided to determine if the ARPC1A loss of function decreased APP degradation similarly to CD2AP loss of function.

To assess whether ARPC1A could hinder APP degradation the same way as the loss of CD2AP, we measured membrane APP degradation by chasing surface proteins bound to biotin for 0, 30, and 60 minutes, where at 0 min, biotin-APP is mainly at the cell membrane, and 30 min and 60 min biotin-APP is expected to undergo endocytosis and degradation at the lysosomes. After the chase, the biotinylated surface proteins are immunoprecipitated, and APP is detected by Western blot. Densitometric quantification of the immunoprecipitated APP bands and total APP, followed by normalization of the APP-Biotin (APP-IP) intensity by the total APP at 0 min, allows determining the extent of APP degradation.

In siControl cells, APP degradation was fast, with only 3% of APP left at 30 and 60 minutes (Figure 3.8A, B). However, APP degradation was slower at 30 minutes in the siCD2AP and siARPC1A cells with 61% and 25% of APP left at 30min respectively, reaching similar levels to the control at 60 minutes. These results indicate that ARPC1A, as CD2AP, regulates the APP endocytic trafficking to the lysosome and when absent, the degradation of APP is decreased.

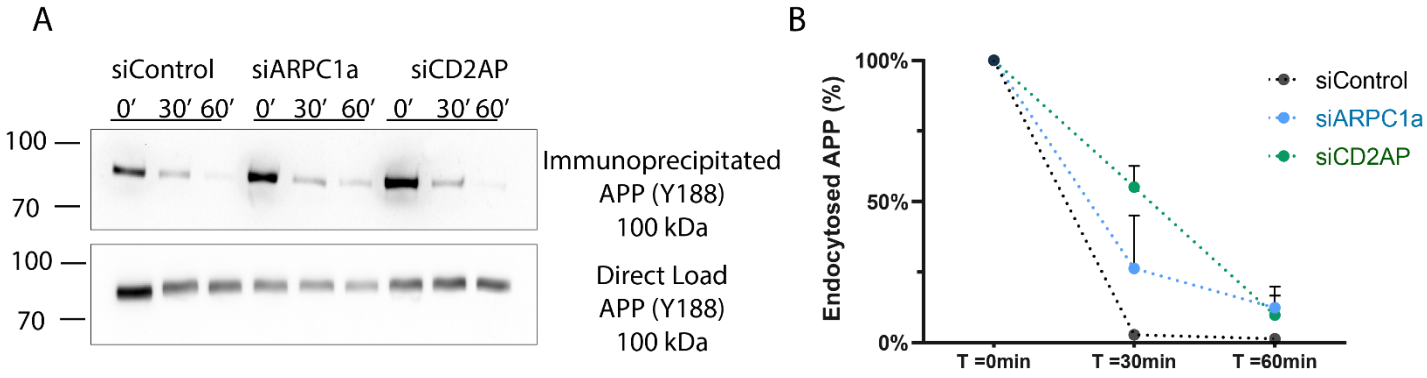

Figure 3.8 ARPC1a regulates APP degradation.

(A) Representative image of Immunoblot for siControl, siARPC1a #3 and siCD2AP. APP was chased for either 0 minutes, 30 minutes, or 60 minutes. Protein immunostained for APP-Y188
(B) Graph with degradation rate of siControl, siARPC1a #3 and siCD2AP over 60 minutes. Levels normalized to 0 minutes of the corresponding condition. (n = 2; mean ± SEM)

V.6 ACTIN AND CD2AP DYNAMICS IN ARPC1A DEPLETED CELLS

Lastly, we decided to assess whether the ARPC1A isoform knockdown could affect the dynamics of CD2AP and F-actin in the perinuclear region. To assess that, we transfected siControl and siARPC1A-treated cells with CD2AP-GFP and LifeAct-mCherry, a small F-actin binding peptide (Riedl et al., 2008). We performed fluorescence recovery after photobleaching (FRAP) for 20 sec, quantifying the recovery of CD2AP and F-actin signals after bleaching a small part of the perinuclear region (Figure 3.9A).

In preliminary experiments, we observed that CD2AP was present in bright puncta in the perinuclear region, bleached efficiently (time zero), and showed a partial recovery after 20 sec in siControl cells. In cells treated with siARPC1A, the CD2AP puncta were less distinguishable from the cytosolic pool of CD2AP, in agreement with our previous observations that siARPC1A reduces CD2AP enrichment in the perinuclear region (Figure 3.5). Differently from siControl cells, the CD2AP-GFP signal bleaching was not as efficient, with some signal remaining at time zero. We could observe partial CD2AP signal recovery 20 sec after photobleaching.

Quantification of CD2AP fluorescence in the photobleached region of siARPC1A-treated cells revealed an inferior recovery than in siControl-treated cells (Figure 3.9A). In contrast, LifeAct fluorescence recovery was superior in siARPC1A-treated cells (Figure 3.9B), indicating a higher turnover of F-actin.

These results suggest that the absence of ARPC1A may lead to higher stability of CD2AP at the perinuclear region. Alternatively, the fast diffusion of free CD2AP during photobleaching might reduce the CD2AP recovery. F-actin recovery may be unexpectedly faster after siARPC1A, indicating that the F-actin left after siARPC1a is less stable than in control cells. Potentially this F-actin dynamicity could be dependent on other actin-binding proteins, such as formins.

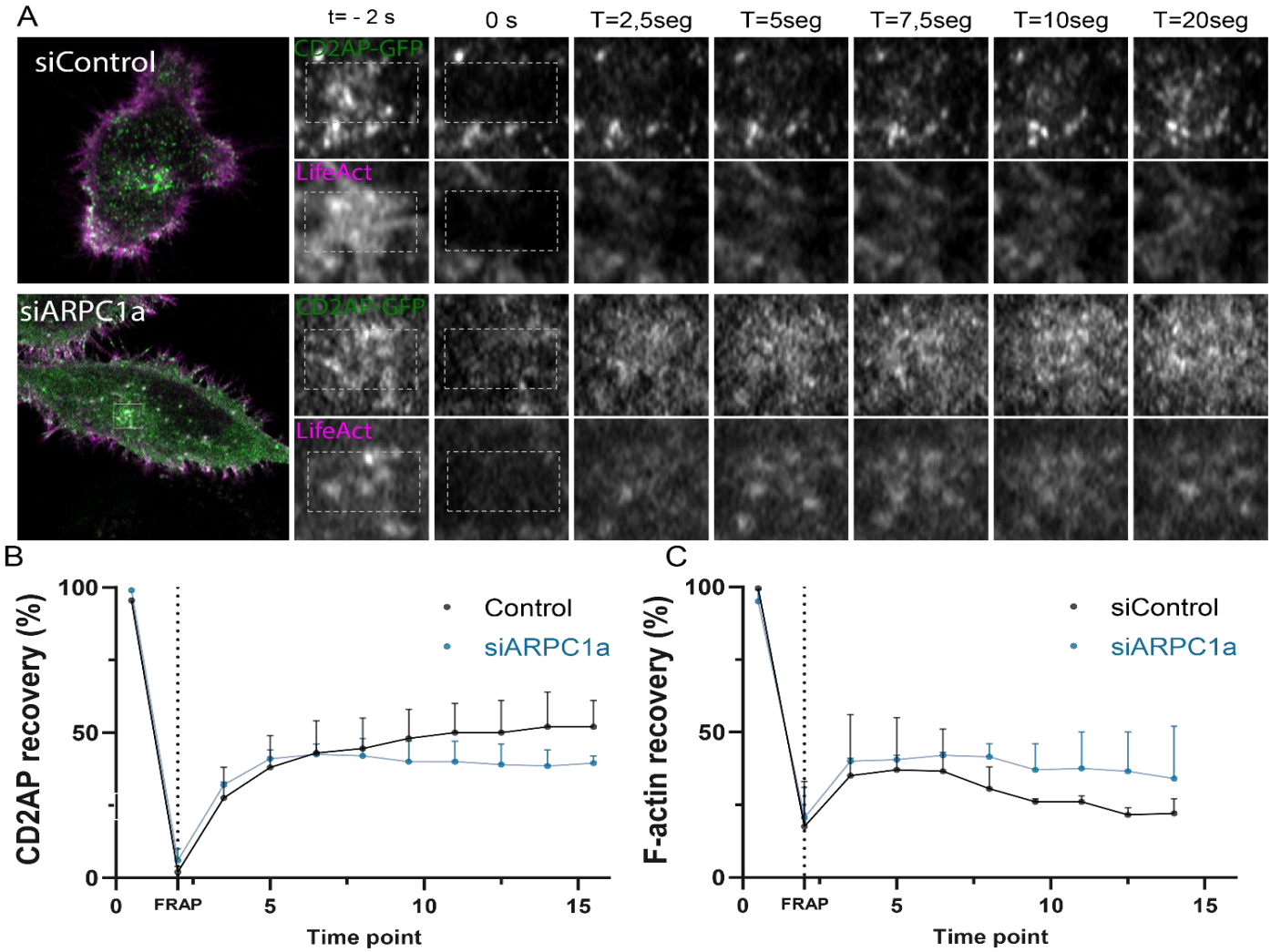

Figure 3.9 Fluorescence Recovery after bleaching of siARPC1A for CD2AP-GFP and LifeAct-Cherry
(**A)** Representative image of control and siARPC1A N2a cells expressing CD2AP-GFP and Life-Act Cherry.
(**B, C)** Graph of CD2AP (**B)** and F-actin (**C**) recovery after photobleaching. Photobleaching was performed 2 seconds after imaging, and recovery was quantified for 15 seconds. (n = 2, N = 12-13 cells; mean ± SEM)

VI. DISCUSSION

CD2AP had previously been reported to regulate the endosomal sorting of APP for degradation and suggested regulating perinuclear F-actin, but whether F-actin remodeling was required for APP sorting was unknown. Here we sought to assess the function of the ARPC1A containing Arp 2/3 complex in regulating the endocytic traffic through actin branch polymerization. Here we report that CD2AP and the ARPC1A containing Arp 2/3 complex are required for F-actin polymerization in the endosomal-rich perinuclear region. Furthermore, ARPC1A depletion decreases the localization of CD2AP to the perinuclear region and affects the endocytic trafficking, delaying the degradation of APP.

F-actin polymerization in the endosomal-rich perinuclear region

Previous work suggested that downregulation of CD2AP decreases perinuclear F-actin. In this work, by performing a rescue experiment, we confirmed the specificity of the siRNA against CD2AP previously used and corroborated that CD2AP is required for maintaining perinuclear F-actin.

Next, we decided to target F-actin polymerization in the perinuclear region independently of CD2AP. In a previous pilot experiment, ARPC1A knockdown reduced perinuclear F-actin, like lack of CD2AP. Indeed, we confirmed the function of ARPC1A in polymerizing F-actin, specifically in the perinuclear region. In agreement, the alternate isoform ARPC1B mainly functions in the cell cortex (Molinie et al., 2019). Thus, the similar phenotype observed between siCD2AP and siARPC1A indicates that both sustain endosomal F-actin. We conclude that the endosomal branched actin depends on ARPC1A for its polymerization and CD2AP for its stabilization, as described *in vitro* (V. W. Tang & Brieher, 2013).

We also noted an increase in the filopodia-like protrusions with the downregulation of CD2AP or ARPC1A. The increase in filopodia-like protrusions could be explained due to the endosomal F-actin depolymerization causing an increased availability of monomeric actin for F-actin polymerization at the cell cortex (Suarez & Kovar, 2016). Alternatively, since capping protein (CP) recruitment to the cell cortex is dependent on CD2AP in podocytes (Jianping Zhao et al., 2013), CD2AP depletion could reduce the capping of cortical F-actin, increasing its polymerization.

ARPC1A capacity to promote the enrichment of CD2AP on endosomes

We found ARPC1A to influence CD2AP localization since CD2AP associates more with ARPC1A than ARPC1B, and its localization to the perinuclear region decreases in the absence of ARPC1A. Since CD2AP binds to F-actin, our results indicate that it may preferentially bind to F-actin polymerized by ARPC1A-containing Arp 2/3 complex. Alternatively, the ARPC1A-containing Arp 2/3 complex may indirectly recruit CD2AP to endosomes via cortactin (Lynch et al., 2003). Indeed, Welsch *et al.* detected CD2AP in cytoplasmatic spots in podocytes, colocalizing with F-actin, cortactin, and the Arp 2/3 complex (Welsch et al., 2005).

Preliminary results suggest decreased CD2AP dynamics in the absence of ARPC1A, indicating a decrease in binding sites for CD2AP on endosomes. Indeed, CD2AP localizes on motile vesicles associated with dynamic actin. Thus, by depleting branched actin polymerization, the decreased CD2AP dynamics could reflect the pool of CD2AP associated with Arp 2/3-independent and more stable F-actin.

As for the increased turnover of F-actin in siARPC1A cells, although unexpected, may be justified by an increased actin polymerization by other actin-binding proteins, namely formins (Ganguly et al., 2015; Gong et al., 2018; Goode & Eck, 2007; Theos et al., 2005). Interestingly, the disassembly of branched actin and Arp 2/3 inhibition was found to shortly increase the pool of free G-actin that rapidly incorporated in linear F-actin, polymerized by formins (Suarez & Kovar, 2016)

ARPC1A impact on APP trafficking

ARPC1A loss of function affected the degradation of APP to a similar extent to CD2AP loss of function. This confirmed previous results from Ubelmann, indicating a delay in APP degradation in siCD2AP cells. The ARPC1A-containing Arp 2/3 complex may aid CD2AP in sorting APP for degradation. Similarly, cortactin (Muriel et al., 2016) and WASH (MacDonald et al., 2018), two CD2AP and Arp 2/3 interactors, regulate receptor degradation and multivesicular body biogenesis.

The reduced endosome size upon siARPC1A and siCD2AP unexpectedly contrasted with previous lab results. One possible explanation could reside in differences in the decrease in the endosomal F-actin caused by siARPC1A or siCD2AP between our experimental conditions. If the knockdown was more efficient than in previous experiments, cortical F-actin could also be affected by decreasing APP endocytosis and early endosome size (Burrinha et al., 2021). Alternatively, this phenotype might result in altering capping protein recruitment to endosomes. Indeed, CapZ is a capping protein found to regulate endosome size and maturation. In CapZ KO cells, endosomal F-actin increases due to a decreased capping activity, and endosomes become larger. Secondly, CapZ interacts with Rab5 effectors through its N-terminal, which docked them to the

early endosomes through the C-terminal capping activity on endosomal F-actin. CapZ KO decreased the colocalization of Rab5 with effectors such as EEA1 (Wang et al., 2021).

Furthermore, vesicle fusion is a process dependent on the transport of vesicles along the cytoskeleton and the activity of tethering factors, such as EEA1 (Gautreau et al., 2014; Gomez et al., 2012; Savvas Christoforidis et al., 1999). With this in mind, the ARPC1A containing complex might have a similar mechanism, promoting branched actin sites for CAPZ binding. The decreased endosome size in siARPC1A-treated cells could result from decreased branched actin polymerization, reducing CapZ and EEA1. Lastly, this would consequently hinder vesicle fusion. Similarly, in CD2AP depleted cells, the decreased size of endosomes could be explained by the interaction between CD2AP and CapZ (Hutchingst et al., 2003), which could affect the localization of CapZ on endosomes and reduce the recruitment of Rab5 effectors.

Finally, Ubelmann *et al*. observed a decrease in APP on endosomes upon siCD2AP treatment, which increased fourfold upon gamma-secretase inhibition, indicating that APP was accumulating in endosomes but disappearing due to processing into Aβ (Ubelmann et al., 2017). Thus, the decreased APP on endosomes in siARPC1A cells similarly results from the increased processing of APP by BACE1 and γ-secretase, decreasing the detection of full-length APP. Results from the lab support this last hypothesis since it was observed that Aβ increases when siARPC1a is knockdown.

VII. CONCLUSION AND FUTURE DIRECTIONS

In this work, we have shown that the ARPC1A isoform regulates APP endocytic trafficking similarly to CD2AP. We found that ARPC1A downregulation decreases perinuclear F-actin and perinuclear CD2AP. Similarly, overexpressing ARPC1A enriches CD2AP on endosomes. When investigating the effects on endocytic trafficking, we found that ARPC1A downregulation affects early endosome size and delays the degradation of APP.

In the future, we pretend to replicate the preliminary experiments obtained, expecting to confirm the observed phenotypes. In addition, while the mechanism of endosomal sorting was studied in N2a cells, we intend to validate the results observed by the ARPC1A loss of function in primary mouse neurons.

Is the CD2AP recruitment to the perinuclear region specific to the ARPC1A isoform? We will investigate whether ARPC1B loss of function similarly impacts the perinuclear and cortical CD2AP. In addition, CD2AP binds cortactin which binds the ARP3/3 complex, and it is known to recruit CD2AP to the cell cortex. Thus, we hypothesize whether cortactin mediates the effects of ARPC1A on CD2AP and APP trafficking. Thus, we are interested in studying whether cortactin acts on endosomes, linking CD2AP to ARPC1A-containing Arp 2/3 complex.

Moreover, we could not successfully assess the effects of siARPC1A cells on APP endosomal sorting. As such, we pretend to inhibit the γ-secretase in cells treated with siRNA against ARPC1A and evaluate defects in APP endosomal sorting and the total levels of APP.

How siARPC1A treatment delay APP degradation is not fully clear as multiple stages of the endocytic pathway can slow down its degradation. As such, we intend to perform a pulse-chase combined with an immunocytochemistry assay, enabling us to visualize the trafficking of APP over time in the early and late endosomal compartments.

With the experiments performed in this work and future works, we hope to establish that the F-actin polymerized by the Arp2/3 complex containing the ARPC1A isoform at early endosomes is the mechanism used by CD2AP to control APP endocytic trafficking relevant for amyloidogenesis and the risk of developing Alzheimer's disease.

VIII. REFERENCES

2020 Alzheimer's disease facts and figures. (2020). *Alzheimer's and Dementia*, *16*(3), 391–460. https://doi.org/10.1002/alz.12068

Abella, J. V. G., Galloni, C., Pernier, J., Barry, D. J., Kjær, S., Carlier, M. F., & Way, M. (2016). Isoform diversity in the Arp2/3 complex determines actin filament dynamics. *Nature Cell Biology*, *18*(1), 76–86. https://doi.org/10.1038/ncb3286

Akin, O., & Mullins, R. D. (2008). Capping Protein Increases the Rate of Actin-Based Motility by Promoting Filament Nucleation by the Arp2/3 Complex. *Cell*, *133*(5), 841–851. https://doi.org/10.1016/j.cell.2008.04.011

Arancio, O. (2020). What Does the APP Family Do in the Brain? *Neuron*, *108*(4), 583–585. https://doi.org/10.1016/j.neuron.2020.11.003

Association, A. (n.d.). *Alzheimer's Association Style Guide*.

Bartus RT, 3rd, D. R., B, B., & AS., L. (1982). The cholinergic hypothesis of geriatric memory dysfunction. In *Science* (Vol. 217, Issue 4558, pp. 408–417).

Benesch, S., Polo, S., Lai, F. P., Anderson, K. I., Stradal, T. E. B., Wehland, J., & Rottner, K. (2005). N-WASP deficiency impairs EGF internalization and actin assembly at clathrin-coated pits. *Journal of Cell Science*, *118*(14), 3103–3115. https://doi.org/10.1242/jcs.02444

Bertram, L., & Tanzi, R. E. (2005). The genetic epidemiology of neurodegenerative disease. *Journal of Clinical Investigation*, *115*(6), 1449–1457. https://doi.org/10.1172/JCI24761

Best, B. P. (2015). Cryoprotectant Toxicity: Facts, Issues, and Questions. *Rejuvenation Research*, *18*(5), 422–436. https://doi.org/10.1089/rej.2014.1656

Braun, G. A., Dear, A. J., Sanagavarapu, K., Zetterberg, H., & Linse, S. (2022). Amyloid-β peptide 37, 38 and 40 individually and cooperatively inhibit amyloid-β 42 aggregation. *Chemical Science*, *13*(8), 2423–2439. https://doi.org/10.1039/d1sc02990h

Burrinha, T., & Cláudia, G. A. (2022). Aging impact on amyloid precursor protein neuronal trafficking. *Current Opinion in Neurobiology*, *73*, 102524. https://doi.org/10.1016/j.conb.2022.102524

Burrinha, T., Martinsson, I., Gomes, R., Terrasso, A. P., Gouras, G. K., & Almeida, C. G. (2021). Upregulation of APP endocytosis by neuronal aging drives amyloid-dependent synapse loss. *Journal of Cell Science*, *134*(9). https://doi.org/10.1242/jcs.255752

Chakrabarti, R., Lee, M., & Higgs, H. N. (2021). Multiple roles for actin in secretory and endocytic pathways. *Current Biology*, *31*(10), R603–R618. https://doi.org/10.1016/j.cub.2021.03.038

Cirrito, J. R., Yamada, K. A., Finn, M. B., Sloviter, R. S., Bales, K. R., May, P. C., Schoepp, D. D., Paul, S. M., Mennerick, S., & Holtzman, D. M. (2005). Synaptic activity regulates interstitial fluid amyloid-β levels in

vivo. *Neuron*, *48*(6), 913–922. https://doi.org/10.1016/j.neuron.2005.10.028

Clague, M. J., & Urbé, S. (2008). Multivesicular bodies. *Current Biology*, *18*(10), R402–R404. https://doi.org/10.1016/j.cub.2008.02.068

Cochran, J. N., Rush, T., Buckingham, S. C., & Roberson, E. D. (2015). The Alzheimer's disease risk factor CD2AP maintains blood–brain barrier integrity. *Human Molecular Genetics*, *24*(23), 6667–6674. https://doi.org/10.1093/hmg/ddv371

Cormont, M., Metón, I., Mari, M., Monzo, P., Keslair, F., Gaskin, C., McGraw, T. E., & Le Marchand-Brustel, Y. (2003). CD2AP/CMS regulates endosome morphology and traffic to the degradative pathway through its interaction with Rab4 and c-Cbl. *Traffic*, *4*(2), 97–112. https://doi.org/10.1034/j.1600-0854.2003.40205.x

Cummings, J. L., & Back, C. (1998). The cholinergic hypothesis of neuropsychiatric symptoms in Alzheimer's disease. *American Journal of Geriatric Psychiatry*, *6*(2 SUPPL.), S64–S78. https://doi.org/10.1097/00019442-199821001-00009

Derivery, E., Sousa, C., Gautier, J. J., Lombard, B., Loew, D., & Gautreau, A. (2009). The Arp2/3 Activator WASH Controls the Fission of Endosomes through a Large Multiprotein Complex. *Developmental Cell*, *17*(5), 712–723. https://doi.org/10.1016/j.devcel.2009.09.010

Duleh, S. N., & Welch, M. D. (2010). WASH and the Arp2/3 complex regulate endosome shape and trafficking. *Cytoskeleton*, *67*(3), 193–206. https://doi.org/10.1002/cm.20437

Dustin, M. L., Olszowy, M. W., Holdorf, A. D., Li, J., Bromley, S., Desai, N., Widder, P., Rosenberger, F., Van Der Merwe, P. A., Allen, P. M., & Shaw, A. S. (1998). A novel adaptor protein orchestrates receptor patterning and cytoskeletal polarity in T-cell contacts. *Cell*, *94*(5), 667–677. https://doi.org/10.1016/S0092-8674(00)81608-6

Estimates of Funding for Various Research, Condition, and Disease Categories (RCDC). (2021). https://report.nih.gov/funding/categorical-spending#/

Furusawa, K., Takasugi, T., Chiu, Y. W., Hori, Y., Tomita, T., Fukuda, M., & Hisanaga, S. ichi. (2019). CD2-associated protein (CD2AP) overexpression accelerates amyloid precursor protein (APP) transfer from early endosomes to the lysosomal degradation pathway. *Journal of Biological Chemistry*, *294*(28), 10886–10899. https://doi.org/10.1074/jbc.RA118.005385

Ganguly, A., Tang, Y., Wang, L., Ladt, K., Loi, J., Dargent, B., Leterrier, C., & Roy, S. (2015). A dynamic formin-dependent deep F-actin network in axons. *Journal of Cell Biology*, *210*(3), 401–417. https://doi.org/10.1083/jcb.201506110

Garrels, J. I., & Gibson, W. (1976). Identification and characterization of multiple forms of actin. *Cell*, *9*(4 PART 2), 793–805. https://doi.org/10.1016/0092-8674(76)90142-2

Gauthier, N. C., Monzo, P., Gonzalez, T., Doye, A., Oldani, A., Gounon, P., Ricci, V., Cormont, M., & Boquet, P.

(2007). Early endosomes associated with dynamic F-actin structures are required for late trafficking of H. pylori VacA toxin. *Journal of Cell Biology*, *177*(2), 343–354. https://doi.org/10.1083/jcb.200609061

Gautreau, A., Oguievetskaia, K., & Ungermann, C. (2014). Function and regulation of the endosomal fusion and fission machineries. *Cold Spring Harbor Perspectives in Biology*, *6*(3), 1–16. https://doi.org/10.1101/cshperspect.a016832

Glenner, G. and Wong, W. C. (1984). Alzheimer's Disease and Downs Syndrome: Sharing of a unique cerebrovascular amyloid fibril protein. *Biochemical and Biophysical Research Communications*, *122*(3), 1131–1135.

Goley, E. D., & Welch, M. D. (2006). The ARP2/3 complex: An actin nucleator comes of age. *Nature Reviews Molecular Cell Biology*, *7*(10), 713–726. https://doi.org/10.1038/nrm2026

Gomez, T. S., & Billadeau, D. D. (2009). A FAM21-Containing WASH Complex Regulates Retromer-Dependent Sorting. *Developmental Cell*, *17*(5), 699–711. https://doi.org/10.1016/j.devcel.2009.09.009

Gomez, T. S., Gorman, J. A., de Narvajas, A. A. M., Koenig, A. O., & Billadeau, D. D. (2012). Trafficking defects in WASH-knockout fibroblasts originate from collapsed endosomal and lysosomal networks. *Molecular Biology of the Cell*, *23*(16), 3215–3228. https://doi.org/10.1091/mbc.e12-02-0101

Gong, T., Yan, Y., Zhang, J., Liu, S., Liu, H., Gao, J., Zhou, X., Chen, J., & Shi, A. (2018). PTRN -1/ CAMSAP promotes CYK -1/formin-dependent actin polymerization during endocytic recycling . *The EMBO Journal*, *37*(9), 1–19. https://doi.org/10.15252/embj.201798556

Goode, B. L., & Eck, M. J. (2007). Mechanism and function of formins in the control of actin assembly. *Annual Review of Biochemistry*, *76*(February), 593–627. https://doi.org/10.1146/annurev.biochem.75.103004.142647

Guimas Almeida, C., Sadat Mirfakhar, F., Perdigão, C., & Burrinha, T. (2018). Impact of late-onset Alzheimer's genetic risk factors on beta-amyloid endocytic production. *Cellular and Molecular Life Sciences*, *75*(14), 2577–2589. https://doi.org/10.1007/s00018-018-2825-9

Gyorgyi, S. (1943). *Muscular Contraction*.

Halliday, M. R., Rege, S. V., Ma, Q., Zhao, Z., Miller, C. A., Winkler, E. A., & Zlokovic, B. V. (2016). Accelerated pericyte degeneration and blood-brain barrier breakdown in apolipoprotein E4 carriers with Alzheimer's disease. *Journal of Cerebral Blood Flow and Metabolism*, *36*(1), 216–227. https://doi.org/10.1038/jcbfm.2015.44

Harbour, M. E., Breusegem, S. Y., & Seaman, M. N. J. (2012). Recruitment of the endosomal WASH complex is mediated by the extended "tail" of Fam21 binding to the retromer protein Vps35. *Biochemical Journal*, *442*(1), 209–220. https://doi.org/10.1042/BJ20111761

Harrison, B. J., Venkat, G., Lamb, J. L., Hutson, T. H., Drury, C., Rau, K. K., Bunge, M. B., Mendell, L. M., Gage, F. H., Johnson, R. D., Hill, C. E., Rouchka, E. C., Moon, L. D. F., & Petruska, J. C. (2016). The adaptor

protein CD2AP is a coordinator of neurotrophin signaling-mediated axon arbor plasticity. *Journal of Neuroscience*, *36*(15), 4259–4275. https://doi.org/10.1523/JNEUROSCI.2423-15.2016

Helfer, E., Harbour, M. E., Henriot, V., Lakisic, G., Sousa-Blin, C., Volceanov, L., Seaman, M. N. J., & Gautreau, A. (2013). Endosomal recruitment of the WASH complex: Active sequences and mutations impairing interaction with the retromer. *Biology of the Cell*, *105*(5), 191–207. https://doi.org/10.1111/boc.201200038

Herman, I. M. (1993). Actin isoforms. *Current Opinion in Cell Biology*, *5*(1), 48–55. https://doi.org/10.1016/S0955-0674(05)80007-9

Hollingworth, P., Harold, D., Sims, R., Gerrish, A., Lambert, C., Carrasquillo, M. M., Abraham, R., Marian, L., Pahwa, J. S., Moskvina, V., Dowzell, K., Stretton, A., Thomas, C., Richards, A., Ivanov, D., Chapman, J., Lovestone, S., Powell, J., Proitsi, P., … Brice, A. (2011). Common variants in ABCA7, MS4A6A/MS4A4E, EPHA1, CD33 and CD2AP are associated with Alzheimer's disease. *Nature Genetics*, *43*(5), 429–435. https://doi.org/10.1038/ng.803.Common

Hutchingst, N. J., Clarkson, N., Chalkley, R., Barclay, A. N., & Brown, M. H. (2003). Linking the T cell surface protein CD2 to the actin-capping protein CAPZ via CMS and CIN85. *Journal of Biological Chemistry*, *278*(25), 22396–22403. https://doi.org/10.1074/jbc.M302540200

Irwin, K., Sexton, C., Daniel, T., Lawlor, B., & Naci, L. (2018). Healthy aging and dementia: Two roads diverging in midlife? *Frontiers in Aging Neuroscience*, *10*(SEP), 1–12. https://doi.org/10.3389/fnagi.2018.00275

Jay, P., Bergé-Lefranc, J. L., Massacrier, A., Roessler, E., Wallis, D., Muenke, M., Gastaldi, M., Taviaux, S., Cau, P., & Berta, P. (2000). ARP3β, the gene encoding a new human actin-related protein, is alternatively spliced and predominantly expressed in brain neuronal cells. *European Journal of Biochemistry*, *267*(10), 2921–2928. https://doi.org/10.1046/j.1432-1327.2000.01306.x

Jin, M., Shirazinejad, C., Wang, B., Yan, A., Schöneberg, J., Upadhyayula, S., Xu, K., & Drubin, D. G. (2022). Branched actin networks are organized for asymmetric force production during clathrin-mediated endocytosis in mammalian cells. *Nature Communications*, *13*(1). https://doi.org/10.1038/s41467-022-31207-5

Kahr, W. H. A., Pluthero, F. G., Elkadri, A., Warner, N., Drobac, M., Chen, C. H., Lo, R. W., Li, L., Li, R., Li, Q., Thoeni, C., Pan, J., Leung, G., Lara-Corrales, I., Murchie, R., Cutz, E., Laxer, R. M., Upton, J., Roifman, C. M., … Muise, A. M. (2017). Loss of the Arp2/3 complex component ARPC1B causes platelet abnormalities and predisposes to inflammatory disease. *Nature Communications*, *8*, 1–14. https://doi.org/10.1038/ncomms14816

Kaksonen, M., Sun, Y., & Drubin, D. G. (2003). A Pathway for Association of Receptors, Adaptors, and Actin during Endocytic Internalization. *Cell*, *115*(4), 475–487. https://doi.org/10.1016/S0092-8674(03)00883-

3

Kamenetz, F., Tomita, T., Hsieh, H., Seabrook, G., Borchelt, D., Iwatsubo, T., Sisodia, S., & Malinow, R. (2003). APP Processing and Synaptic Function. *Neuron*, *37*(6), 925–937. https://doi.org/10.1016/S0896-6273(03)00124-7

Kayed, R., Head, E., Thompson, J. L., McIntire, T. M., Milton, S. C., Cotman, C. W., & Glabel, C. G. (2003). Common structure of soluble amyloid oligomers implies common mechanism of pathogenesis. *Science*, *300*(5618), 486–489. https://doi.org/10.1126/science.1079469

Keating, D. M. R. and G. M. (2011). Memantine. *Nihon Rinsho. Japanese Journal of Clinical Medicine*, *69 Suppl 1*(Pt 2), 41–46. https://doi.org/10.12968/jprp.2021.3.8.298

Kim, J., Basak, J. M., & Holtzman, D. M. (2011). The Role of Apolipoprotein E in Alzheimer's Disease. *Neuron*, *63*(3), 287–303. https://doi.org/10.1016/j.neuron.2009.06.026.The

Kinley, A. W., Weed, S. A., Weaver, A. M., Karginov, A. V., Bissonette, E., Cooper, J. A., & Parsons, J. T. (2003). Cortactin interacts with WIP in regulating Arp2/3 activation and membrane protrusion. *Current Biology*, *13*(5), 384–393. https://doi.org/10.1016/S0960-9822(03)00107-6

Kirsch, K. H., Georgescu, M. M., Ishimaru, S., & Hanafusa, H. (1999). CMS: An adapter molecule involved in cytoskeletal rearrangements. *Proceedings of the National Academy of Sciences of the United States of America*, *96*(11), 6211–6216. https://doi.org/10.1073/pnas.96.11.6211

Kobayashi, N. (2002). Mechanism of the process formation; podocytes vs. neurons. *Microscopy Research and Technique*, *57*(4), 217–223. https://doi.org/10.1002/jemt.10077

Koo, E. H., & Squazzo, S. L. (1994). Evidence that production and release of amyloid β-protein involves the endocytic pathway. *Journal of Biological Chemistry*, *269*(26), 17386–17389. https://doi.org/10.1016/s0021-9258(17)32449-3

Kunkle, B. W., Grenier-Boley, B., Sims, R., Bis, J. C., Damotte, V., Naj, A. C., Boland, A., Vronskaya, M., van der Lee, S. J., Amlie-Wolf, A., Bellenguez, C., Frizatti, A., Chouraki, V., Martin, E. R., Sleegers, K., Badarinarayan, N., Jakobsdottir, J., Hamilton-Nelson, K. L., Moreno-Grau, S., … Pericak-Vance, M. A. (2019). Genetic meta-analysis of diagnosed Alzheimer's disease identifies new risk loci and implicates Aβ, tau, immunity and lipid processing. *Nature Genetics*, *51*(3), 414–430. https://doi.org/10.1038/s41588-019-0358-2

LaFerla, F. M., Green, K. N., & Oddo, S. (2007). Intracellular amyloid-β in Alzheimer's disease. *Nature Reviews Neuroscience*, *8*(7), 499–509. https://doi.org/10.1038/nrn2168

Lalli, G., Schott, J. M., Hardy, J., & De Strooper, B. (2021). Aducanumab: a new phase in therapeutic development for Alzheimer's disease? *EMBO Molecular Medicine*, *13*(8), 2–4. https://doi.org/10.15252/emmm.202114781

Lambert, J. C., Ibrahim-Verbaas, C. A., Harold, D., Naj, A. C., Sims, R., Bellenguez, C., Jun, G., DeStefano, A. L.,

Bis, J. C., Beecham, G. W., Grenier-Boley, B., Russo, G., Thornton-Wells, T. A., Jones, N., Smith, A. V., Chouraki, V., Thomas, C., Ikram, M. A., Zelenika, D., … Seshadri, S. (2013). Meta-analysis of 74,046 individuals identifies 11 new susceptibility loci for Alzheimer's disease. *Nature Genetics*, *45*(12), 1452–1458. https://doi.org/10.1038/ng.2802

Lee, S. H., Kang, J., Ho, A., Watanabe, H., Bolshakov, V. Y., & Shen, J. (2020). APP Family Regulates Neuronal Excitability and Synaptic Plasticity but Not Neuronal Survival. *Neuron*, *108*(4), 676-690.e8. https://doi.org/10.1016/j.neuron.2020.08.011

LI, C., RUOTSALAINEN, V., TRYGGVASON, K., SHAW, A. S., MINER1, & H., J. (2000). CD2AP is expressed with nephrin in developing podocytes and is found widely in mature kidney and elsewhere. *International Journal of Radiation Biology*, *57*(5), 939–946. https://doi.org/10.1080/09553009014551061

Ludewig, S., & Korte, M. (2017). Novel insights into the physiological function of the APP (GENE) family and its proteolytic fragments in synaptic plasticity. *Frontiers in Molecular Neuroscience*, *9*(January), 1–15. https://doi.org/10.3389/fnmol.2016.00161

Lynch, D. K., Winata, S. C., Lyons, R. J., Hughes, W. E., Lehrbach, G. M., Wasinger, V., Corthals, G., Cordwell, S., & Daly, R. J. (2003). A cortactin-CD2-associated protein (CD2AP) complex provides a novel link between epidermal growth factor receptor endocytosis and the actin cytoskeleton. *Journal of Biological Chemistry*, *278*(24), 21805–21813. https://doi.org/10.1074/jbc.M211407200

MacDonald, E., Brown, L., Selvais, A., Liu, H., Waring, T., Newman, D., Bithell, J., Grimes, D., Urbé, S., Clague, M. J., & Zech, T. (2018). HRS-WASH axis governs actin-mediated endosomal recycling and cell invasion. *Journal of Cell Biology*, *217*(7), 2549–2564. https://doi.org/10.1083/jcb.201710051

Mario F. Mendez, M.D., P. D. (2018). Early-Onset Alzheimer's Disease Mario. *Neurologic Clinics*, *72*(23), 2964–2979. https://doi.org/10.1016/j.ncl.2017.01.005.Early-Onset

Masters, C. L., Simms, G., Weinman, N. A., Multhaup, G., McDonald, B. L., & Beyreuther, K. (1985). Amyloid plaque core protein in Alzheimer disease and Down syndrome. *Proceedings of the National Academy of Sciences of the United States of America*, *82*(12), 4245–4249. https://doi.org/10.1073/pnas.82.12.4245

Mdawar, B., Ghossoub, E., & Khoury, R. (2020). Selective serotonin reuptake inhibitors and Alzheimer's disease. *Neural Regeneration Research*, *15*(1), 41–46. https://doi.org/10.4103/1673-5374.264445

Merrifield, C. J., Perrais, D., & Zenisek, D. (2005). Coupling between clathrin-coated-pit invagination, cortactin recruitment, and membrane scission observed in live cells. *Cell*, *121*(4), 593–606. https://doi.org/10.1016/j.cell.2005.03.015

Molinie, N., Rubtsova, S. N., Fokin, A., Visweshwaran, S. P., Rocques, N., Polesskaya, A., Schnitzler, A., Vacher, S., Denisov, E. V., Tashireva, L. A., Perelmuter, V. M., Cherdyntseva, N. V., Bièche, I., & Gautreau, A. M. (2019). Cortical branched actin determines cell cycle progression. *Cell Research*, *29*(6), 432–445. https://doi.org/10.1038/s41422-019-0160-9

Montagna, E., Dorostkar, M. M., & Herms, J. (2017). The role of APP in structural spine plasticity. *Frontiers in Molecular Neuroscience*, *10*(May), 1–7. https://doi.org/10.3389/fnmol.2017.00136

Monzo, P., Mari, M., Kaddai, V., Gonzalez, T., Le Marchand-Brustel, Y., & Cormont, M. (2005). CD2AP, Rabip4, and Rabip4': Analysis of Interaction with Rab4a and regulation of endosomes morphology. *Methods in Enzymology*, *403*(2000), 107–118. https://doi.org/10.1016/s0076-6879(05)03010-7

Moreau, V., & Winsor, B. (1997). The Yeast Actin-related Protein Arp2p Is Required for the Internalization Step of Endocytosis. *Molecular Biology of the Cell*, *8*(July), 1361–1375.

Mukhopadhyay, S., Banerjee, D., & Kosagisharaf, J. R. (2021). A Primer on the Evolution of Aducanumab: The First Antibody Approved for Treatment of Alzheimer's Disease. *Journal of Alzheimer's Disease*, *83*(4), 1537–1552. https://doi.org/10.3233/JAD-215065

Müller, U. C., Deller, T., & Korte, M. (2017). Not just amyloid: Physiological functions of the amyloid precursor protein family. *Nature Reviews Neuroscience*, *18*(5), 281–298. https://doi.org/10.1038/nrn.2017.29

Müller, U. C., & Zheng, H. (2012). Physiological functions of APP family proteins. *Cold Spring Harbor Perspectives in Medicine*, *2*(2), 1–17. https://doi.org/10.1101/cshperspect.a006288

Muriel, O., Tomas, A., Scott, C. C., & Gruenberg, J. (2016). Moesin and cortactin control actin-dependent multivesicular endosome biogenesis. *Molecular Biology of the Cell*, *27*(21), 3305–3316. https://doi.org/10.1091/mbc.E15-12-0853

Mustonen, H., Lepistö, A., Lehtonen, S., Lehtonen, E., Puolakkainen, P., & Kivilaakso, E. (2005). CD2AP contributes to cell migration and adhesion in cultured gastric epithelium. *Biochemical and Biophysical Research Communications*, *332*(2), 426–432. https://doi.org/10.1016/j.bbrc.2005.04.140

O'Brien, R. J., & Wong, P. C. (2011). Amyloid precursor protein processing and alzheimer's disease. *Annual Review of Neuroscience*, *34*, 185–204. https://doi.org/10.1146/annurev-neuro-061010-113613

Oh, E. S., & Troncoso, J. C. (2014). APP Family Regulates Neuronal Excitability and Synaptic Plasticity but Not Neuronal Survival. *Bone*, *23*(1), 1–7. https://doi.org/10.1016/j.neurobiolaging.2007.12.024.Amyloid

Ojelade, S. A., & M., J. (2019). cindr, the Drosophila Homolog of the CD2AP Alzheimer's Disease Risk Gene, Is Required for Synaptic Transmission and Proteostasis. *Physiology & Behavior*, *176*(3), 139–148. https://doi.org/10.1016/j.celrep.2019.07.041.cindr

Pawson, T., & Scott, J. D. (1997). Signaling through scaffold, anchoring, and adaptor proteins. *Science*, *278*(5346), 2075–2080. https://doi.org/10.1126/science.278.5346.2075

Pollard, T. D. (2016). Actin and actin-binding proteins. *Cold Spring Harbor Perspectives in Biology*, *8*(8), 1–17. https://doi.org/10.1101/cshperspect.a018226

Rabinovici, B. G. D. (2019). *Late-onset Alzheimer Disease*. *February*, 14–33.

Reinhard, C., Hébert, S. S., & De Strooper, B. (2005). The amyloid-β precursor protein: Integrating structure

with biological function. *EMBO Journal*, *24*(23), 3996–4006. https://doi.org/10.1038/sj.emboj.7600860

Riedl, J., Crevenna, A. H., Kessenbrock, K., Yu, J. H., Neukirchen, D., Bista, M., Bradke, F., Jenne, D., Holak, T. A., Werb, Z., Sixt, M., & Wedlich-Soldner, R. (2008). Lifeact: A versatile marker to visualize F-actin. *Nature Methods*, *5*(7), 605–607. https://doi.org/10.1038/nmeth.1220

Rottner, K., Faix, J., Bogdan, S., Linder, S., & Kerkhoff, E. (2017). Actin assembly mechanisms at a glance. *Journal of Cell Science*, *130*(20), 3427–3435. https://doi.org/10.1242/jcs.206433

Rouka, E., Simister, P. C., Janning, M., Kumbrink, J., Konstantinou, T., Muniz, J. R. C., Joshi, D., O'Reilly, N., Volkmer, R., Ritter, B., Knapp, S., Von Delft, F., Kirsch, K. H., & Feller, S. M. (2015). Differential recognition preferences of the three Src Homology 3 (SH3) domains from the adaptor CD2-associated Protein (CD2AP) and Direct Association with Ras and Rab Interactor 3 (RIN3). *Journal of Biological Chemistry*, *290*(42), 25275–25292. https://doi.org/10.1074/jbc.M115.637207

Salas-Cortes, L., Ye, F., Tenza, D., Wilhelm, C., Theos, A., Louvard, D., Raposo, G., & Coudrier, E. (2005). Myosin lb modulates the morphology and the protein transport within multi-vesicular sorting endosomes. *Journal of Cell Science*, *118*(20), 4823–4832. https://doi.org/10.1242/jcs.02607

Savvas Christoforidis, Heidi M. McBride, Robert D. Burgoyne, & Marino Zerial. (1999). The Rab5 effector EEA1is a core componentof endosome docking. *Nature*, *397*(February), 621–625.

Schaerer-Brodbeck, C., & Riezman, H. (2000). Functional interactions between the p35 subunit of the Arp2/3 complex and calmodulin in yeast. *Molecular Biology of the Cell*, *11*(4), 1113–1127. https://doi.org/10.1091/mbc.11.4.1113

Schmidt, A., & Hall, M. (1998). Signaling to the Actin Cytoskeleton. *Cell Development Biology*.

Schneider, L. (2020). A resurrection of aducanumab for Alzheimer's disease. *The Lancet Neurology*, *19*(2), 111–112. https://doi.org/10.1016/S1474-4422(19)30480-6

Schorer, C. E. (1985). Historical essay: Kraepelin's description of Alzheimer's disease. *International Journal of Aging & Human Development*, *21*(3), 235–238. https://doi.org/10.2190/gnq1-gdux-eptl-0f2l

Selkoe DJ. (1998). The cell biology of beta-amyloid precursor protein and presenilin in Alzheimer's disease. *Trends in Cell Biology*, *8*(11), 447–453.

Sepehry, A. A., Lee, P. E., Hsiung, G. Y. R., Beattie, B. L., & Jacova, C. (2012). Effect of selective serotonin reuptake inhibitors in Alzheimer's disease with Comorbid depression: A meta-analysis of depression and cognitive outcomes. *Drugs and Aging*, *29*(10), 793–806. https://doi.org/10.1007/s40266-012-0012-5

Seubert, P., Oltersdorf, T., Lee, M. G., Barbour, R., Blomquist, C., Davis, D. L., Bryant, K., Fritz, L. C., Galasko, D., Thal, L. J., Lieberburg, I., & Schenk, D. B. (1993). Secretion of β-amyloid precursor protein cleaved at the amino terminus of the β-amyloid peptide. *Nature*, *361*(6409), 260–263. https://doi.org/10.1038/361260a0

Shen, R., Zhao, X., He, L., Ding, Y., Xu, W., Lin, S., Fang, S., Yang, W., Sung, K., Spencer, B., Rissman, R. A., Lei, M., Ding, J., & Wu, C. (2020). Upregulation of RIN3 induces endosomal dysfunction in Alzheimer's disease. *Translational Neurodegeneration*, *9*(1). https://doi.org/10.1186/s40035-020-00206-1

Small, S., & Gandy, S. (2006). Sorting through the Cell Biology of Alzheimer's Disease: Intracellular Pathways to Pathogenesis. *Neuron*, *176*(1), 139–148. https://doi.org/10.1016/j.neuron.2006.09.001.Sorting

Stelzmann, R. A., Norman Schnitzlein, H., & Reed Murtagh, F. (1995). An english translation of alzheimer's 1907 paper, "über eine eigenartige erkankung der hirnrinde." *Clinical Anatomy*, *8*(6), 429–431. https://doi.org/10.1002/ca.980080612

Strober, W. (2001). Trypan blue exclusion test of cell viability. *Current Protocols in Immunology / Edited by John E. Coligan ... [et Al.]*, *Appendix 3*, 2–3. https://doi.org/10.1002/0471142735.ima03bs21

Suarez, C., & Kovar, D. R. (2016). Internetwork competition for monomers governs actin cytoskeleton organization. *Nature Reviews Molecular Cell Biology*, *176*(10), 139–148. https://doi.org/10.1038/nrm.2016.106.Internetwork

Sweeney, M. D., Sagare, A. P., & Zlokovic, B. V. (2018). Blood-brain barrier breakdown in Alzheimer disease and other neurodegenerative disorders. *Nature Reviews Neurology*, *14*(3), 133–150. https://doi.org/10.1038/nrneurol.2017.188

Tang, B. L. (2009). Neuronal protein trafficking associated with Alzheimer disease: From APP and BACE1 to glutamate receptors. *Cell Adhesion and Migration*, *3*(1), 118–128. https://doi.org/10.4161/cam.3.1.7254

Tang, V. W., & Brieher, W. M. (2013). FSGS3/CD2AP is a barbed-end capping protein that stabilizes actin and strengthens adherens junctions. *Journal of Cell Biology*, *203*(5), 815–833. https://doi.org/10.1083/jcb.201304143

Theos, A. C., Martina, A., Hurbain, I., Peden, A. A., Sviderskaya, E. V, Stewart, A., Robinson, M. S., Bennett, D. C., Cutler, D. F., Bonifacino, J. S., & Marks, M. S. (2005). Functions of adaptor protein (AP)-3 and AP-1 in tyrosinase sorting from endosomes to melanosomes. *Molecular Biology of the Cell*, *16*(November), 5356–5372. https://doi.org/10.1091/mbc.E05

Tremblay, R. G., Sikorska, M., Sandhu, J. K., Lanthier, P., Ribecco-Lutkiewicz, M., & Bani-Yaghoub, M. (2010). Differentiation of mouse Neuro 2A cells into dopamine neurons. *Journal of Neuroscience Methods*, *186*(1), 60–67. https://doi.org/10.1016/j.jneumeth.2009.11.004

Ubelmann, F., Burrinha, T., Salavessa, L., Gomes, R., Ferreira, C., Moreno, N., & Guimas Almeida, C. (2017). Bin1 and CD 2 AP polarise the endocytic generation of beta-amyloid . *EMBO Reports*, *18*(1), 102–122. https://doi.org/10.15252/embr.201642738

Vadukul, D. M., Gbajumo, O., Marshall, K. E., & Serpell, L. C. (2017). Amyloidogenicity and toxicity of the reverse and scrambled variants of amyloid-β 1-42. *FEBS Letters*, *591*(5), 822–830.

https://doi.org/10.1002/1873-3468.12590

Van Cauwenberghe, C., Van Broeckhoven, C., & Sleegers, K. (2016). The genetic landscape of Alzheimer disease: Clinical implications and perspectives. *Genetics in Medicine*, *18*(5), 421–430. https://doi.org/10.1038/gim.2015.117

Vardarajan, B. N., Ghani, M., Kahn, A., Sheikh, S., Sato, C., Barral, S., Lee, J. H., Cheng, R., Reitz, C., Lantigua, R., Reyes-Dumeyer, D., Medrano, M., Jimenez-Velazquez, I. Z., Rogaeva, E., St George-Hyslop, P., & Mayeux, R. (2015). Rare coding mutations identified by sequencing of Alzheimer disease genome-wide association studies loci. *Annals of Neurology*, *78*(3), 487–498. https://doi.org/10.1002/ana.24466

Wang, D., Ye, Z., Wei, W., Yu, J., Huang, L., Zhang, H., & Yue, J. (2021). Capping protein regulates endosomal trafficking by controlling f-actin density around endocytic vesicles and recruiting rab5 effectors. *ELife*, *10*, 1–25. https://doi.org/10.7554/eLife.65910

Welsch, T., Endlich, N., Gökce, G., Doroshenko, E., Simpson, J. C., Kriz, W., Shaw, A. S., & Endlich, K. (2005). Association of CD2AP with dynamic actin on vesicles in podocytes. *American Journal of Physiology - Renal Physiology*, *289*(5 58-5), 1134–1143. https://doi.org/10.1152/ajprenal.00178.2005

Wendland, B., Emr, S. D., & Riezman, H. (1998). Protein traffic in the yeast endocytic and vacuolar protein sorting pathways. *Current Opinion in Cell Biology*, *10*(4), 513–522. https://doi.org/10.1016/S0955-0674(98)80067-7

Wolf, G., & Stahl, R. A. K. (2003). CD2-associated protein and glomerular disease. *Lancet*, *362*(9397), 1746–1748. https://doi.org/10.1016/S0140-6736(03)14856-8

Yang, B., Parsha, K., Schaar, K., Xi, X., Aronowski, J., & Savitz, S. (2016). Anterograde transport of Rab4-associated vesicles regulates synapse organization in Drosophila. *Physiology & Behavior*, *176*(1), 139–148. https://doi.org/10.1016/j.celrep.2017.02.034.Anterograde

Yiannopoulou, K. G., & Papageorgiou, S. G. (2013). Current and future treatments for Alzheimer's disease. *Therapeutic Advances in Neurological Disorders*, *6*(1), 19–33. https://doi.org/10.1177/1756285612461679

Zhagn, L., & Li, Z. (2014). Alzheimer and the discovery of Alzheimer's disease. *Zhonghua Yi Shi Za Zhi (Beijing, China : 1980)*, *44*(5), 288–290.

Zhao, Jianping, Bruck, S., Cemerski, S., Zhang, L., Butler, B., Dani, A., Cooper, J. A., & Shaw, A. S. (2013). CD2AP Links Cortactin and Capping Protein at the Cell Periphery To Facilitate Formation of Lamellipodia. *Molecular and Cellular Biology*, *33*(1), 38–47. https://doi.org/10.1128/mcb.00734-12

Zhao, Jun, Paganini, L., Mucke, L., Gordon, M., Refolo, L., Carman, M., Sinha, S., Oltersdorf, T., Lieberburg, I., & McConlogue, L. (1996). β-Secretase processing of the β-amyloid precursor protein in transgenic mice is efficient in neurons but inefficient in astrocytes. *Journal of Biological Chemistry*, *271*(49), 31407–31411. https://doi.org/10.1074/jbc.271.49.31407